

# Lipid phosphorylation by a diacylglycerol kinase suppresses ABA biosynthesis to regulate plant stress responses

Jianwu Li<sup>1,2,3</sup>, Shuaibing Yao<sup>1,2,3</sup>, Sang-Chul Kim<sup>1,2</sup> and Xuemin Wang<sup>1,2,\*</sup>

https://doi.org/10.1016/j.molp.2024.01.003

# **ABSTRACT**

Lipid phosphorylation by diacylglycerol kinase (DGK) that produces phosphatidic acid (PA) plays important roles in various biological processes, including stress responses, but the underlying mechanisms remain elusive. Here, we show that DGK5 and its lipid product PA suppress ABA biosynthesis by interacting with ABA-DEFICIENT 2 (ABA2), a key ABA biosynthesis enzyme, to negatively modulate plant response to abiotic stress tested in Arabidopsis thaliana. Loss of DGK5 function rendered plants less damaged, whereas overexpression (OE) of DGK5 enhanced plant damage to water and salt stress. The dgk5 mutant plants exhibited decreased total cellular and nuclear levels of PA with increased levels of diacylglycerol, whereas DGK5-OE plants displayed the opposite effect. Interestingly, we found that both DGK5 and PA bind to the ABA-synthesizing enzyme ABA2 and suppress its enzymatic activity. Consistently, the dgk5 mutant plants exhibited increased levels of ABA, while DGK5-OE plants showed reduced ABA levels. In addition, we showed that both DGK5 and ABA2 are detected in and outside the nuclei, and loss of DGK5 function decreased the nuclear association of ABA2. We found that both DGK5 activity and PA promote nuclear association of ABA2. Taken together, these results indicate that both DGK5 and PA interact with ABA2 to inhibit its enzymatic activity and promote its nuclear sequestration, thereby suppressing ABA production in response to abiotic stress. Our study reveals a sophisticated mechanism by which DGK5 and PA regulate plant stress responses.

Key words: diacylglycerol kinase, phosphatidic acid, diacylglycerol, lipid signaling, stress responses, lipid-protein binding, protein-protein interaction, *Arabidopsis* 

Li J., Yao S., Kim S.-C., and Wang X. (2024). Lipid phosphorylation by a diacylglycerol kinase suppresses ABA biosynthesis to regulate plant stress responses. Mol. Plant. 17, 342–358.

## INTRODUCTION

Lipid phosphorylation catalyzed by diacylglycerol kinases (DGKs) plays crucial roles in biological processes. DGKs in metazoans are involved in a wide range of physiological and pathological processes, including immune response, brain and heart pathology, insulin resistance, and tumor progression (Zha et al., 2006; Chibalin et al., 2008; Dominguez et al., 2013; Sim et al., 2020; Sakane et al., 2021; Bozelli and Epand, 2022). DGKs in plants affect plant growth, development, and stress responses (Go' mez-Merin et al., 2005; Tan et al., 2018; Yuan et al., 2019; Angkawijaya et al., 2020; Wong et al., 2020). Genome-wide analyses of various plant species, including soybean, rice, wheat, and *Arabidopsis*, implicated DGKs in plant responses to different stress conditions (Ge et al., 2012; Cacas et al., 2017; Escobar-

Sepu' Iveda et al., 2017; Tang et al., 2020). Genetic alterations of specific *DGK*s, such as *DGK5*, document the role of DGKs in stress responses, such as responses to freezing and *Pseudomonas syringae* infection in *Arabidopsis* (Tan et al., 2018; Kalachova et al., 2022). However, the precise mechanism underlying DGK actions in plant stress responses remains elusive.

DGK catalyzes the phosphorylation of diacylglycerol (DAG) to form phosphatidic acid (PA) that is an important class of cellular mediators (reviewed in Kim and Wang, 2020; Frias et al., 2023).

Published by the Molecular Plant Shanghai Editorial Office in association with Cell Press, an imprint of Elsevier Inc., on behalf of CSPB and CEMPS, CAS.

<sup>&</sup>lt;sup>1</sup>Department of Biology, University of Missouri-St. Louis, St. Louis, MO 63121, USA

<sup>&</sup>lt;sup>2</sup>Donald Danforth Plant Science Center, St. Louis, MO 63132, USA

<sup>&</sup>lt;sup>3</sup>These authors contributed equally to this article.

<sup>\*</sup>Correspondence: Xuemin Wang (swang@danforthcenter.org)

PA is a minor component of membrane lipids, but its cellular level changes rapidly and transiently in response to various stressors in plants (Welti et al., 2002; Zhang et al., 2004; Vu et al., 2014; Li et al., 2019). PA has been found to bind to proteins involved in various biological processes in plants, animals, and microbes (Kim and Wang, 2020; Kolesnikov et al., 2022; Frias et al., 2023). In addition to DGKs, phospholipase D (PLD) is another major enzyme to produce regulatory PA. Among 12 PLDs in Arabidopsis, many of them are activated and hydrolyze membrane phospholipids to generate PA under stress conditions (Zhang et al., 2004; Vu et al., 2014; Hong et al., 2016). For example, PLDa1 and PLDd have been identified to produce PA that interacts with specific proteins involved in abscisic acid (ABA) signaling and plant stress responses (Zhang et al., 2004, 2009; Li et al., 2019; Kim et al., 2022). However, the direct molecular target of DGKs and their derived PA remains unknown.

ABA is a crucial plant hormone in plant responses to various stress conditions, as well as in plant growth and development. The major ABA biosynthetic pathway in Arabidopsis begins with the epoxidation of zeaxanthin by ABA-DEFICIENT 1 (ABA1), leading to the formation of xanthoxin, which is converted to abscisic aldehyde by ABA2, a short-chain alcohol dehydrogenase (Rook et al., 2001; Gonza' lez-Guzma' n et al., 2002). The resulting abscisic aldehyde is further modified by ABA3 and ABSCISIC ALDEHYDE OXIDASE 3 (AAO3) to produce ABA. In addition, there is an alternative ABA synthesis pathway that is independent of zeaxanthin epoxidation (Jia et al., 2022). ABA2 is encoded by a single-copy gene in Arabidopsis, and ABA2 null mutants exhibit approximately 20% of the ABA content in the wild type (WT), indicating that ABA2-catalyzed reaction is part of the main ABA biosynthetic pathway (Rook et al., 2001; Gonza' lez-Guzma' n et al., 2002). During vegetative growth, the ABA-deficient mutant aba2 plants display stunted root and above-ground growth and increased sensitivity to stress, such as drought and salinity (Lin et al., 2007).

Plant DGKs fall into three phylogenetic clusters (I-III) based on the conserved catalytic kinase domain and the transmembrane helix (Ge et al., 2012; Cacas et al., 2017). The seven DGKs in Arabidopsis are grouped into clusters I (DGK1 and 2), II (DGK3, 4, and 7), and III (DGK5 and 6). Among them, DGK5 has been implicated in plant stress responses based on genome-wide analyses of various plant species and genetic alterations in Arabidopsis (Ge et al., 2012; Cacas et al., 2017; Escobar-Sepu' Iveda et al., 2017; Tan et al., 2018; Tang et al., 2020; Kalachova et al., 2022). In addition, DGK5 has been documented to phosphorylate DAG to PA and is associated with the plasma membrane, cytoplasm, and nucleus (Kalachova et al., 2022). This nuclear association is enticing because DGK5 could potentially impact the nuclear homeostasis of DAG and PA, and recent studies indicate that PA regulates nuclear functions, such as transcription and nuclear translocation of cytosolic proteins in stress responses (Kim et al., 2019; 2022; Cai et al., 2020; Li et al., 2023). However, there is yet no direct evidence for DGK effects on nuclear PA and DAG levels. Here, we show that DGK5 has profound impacts on nuclear PA and DAG levels and, moreover, that DGK5 and PA interact with ABA2 to regulate ABA production and plant stress responses.

## **RESULTS**

DGK5 negatively affects *Arabidopsis* growth under water and NaCl stress

To facilitate functional studies of DGK5 (AT2G20900), we identified two independent T-DNA insertional mutants. dak5-2 with the insertion at 5° UTR (202 bp upstream of the start codon) and dgk5-3 with the insertion at the first exon (46 bp downstream of the start codon) (supplemental Figure 1A). The T-DNA insertions were verified by PCR using primers flanking the T-DNA insertion sites and genomic DNA from dgk5-2 and dgk5-3 (supplemental Figure 1B). The level of DGK5 transcript was negligible in both mutants as evaluated by reverse transcription quantitative-PCR (RT-qPCR) in Arabidopsis plants (Figure 1A). In addition, we genetically complemented dgk5-2 by introducing a native DGK5 genomic sequence with its own promoter into the mutants (supplemental Figure 1C), and the complemented plants, designated as COM, had a similar level of the DGK5 transcript as that in WT (Figure 1A). Furthermore, we overexpressed DGK5 in Arabidopsis under the control of the 35S promoter (supplemental Figure 1D). The DGK5 transcript in two DGK5-overexpression (OE) lines was increased by 15- to 20-fold (Figure 1A), and the production of DGK5 protein was detected by immunoblotting in multiple Arabidopsis OE lines (Figure 1B).

To examine the effect of DGK5 on plant stress responses, we grew DGK5-altered and WT seedlings under water and salt stress conditions (Figure 1; supplemental Figure 2). Without applied stress, the dgk5 mutant and WT plants grew similarly, whereas DGK5-OE plants were smaller than WT and the dgk5 mutant plants (supplemental Figure 2). Under all stress conditions tested, however, the dgk5 mutant plants grew better, whereas DGK5-OE performed worse than WT (Figure 1C and 1D; supplemental Figure 2A and 2B). After withholding water for 16 days followed by resuming watering, up to 70% of the dgk5 mutant plants and 55% of WT plants survived, whereas less than 40% of OE plants survived (Figure 1C, right panel). Under waterlogging, the dry matter was approximately 80% in the dgk5 mutant plants, 60% in WT, and 50% in OE plants after waterlogging for 14 days when compared within each genotype without stress (supplemental Figure 2C). After growing plants under 100 mM NaCl for 14 days, the decrease in growth of the dgk5 mutant plants was much less, whereas that of DGK5-OE was more than that of WT (Figure 1D, right panel). The stress effects on WT and DGK5-altered lines were calculated against respective lines without stress because the growth of DGK5-OE was suppressed without stress (supplemental Figure 2). The opposite effects of the dgk5 mutant and OE were also observed on primary root growth under stress (supplemental Figure 3). The primary root length was comparable among WT, COM, dgk5-2, dgk5-3, and DGK5-OE seedlings without stress. However, in the presence of 75 mM NaCl, 100 mM NaCl, or 150 mM sorbitol, the primary roots were longer in dgk5-2 and dgk5-3, but shorter in DGK5-OE than WT and COM seedlings (supplemental Figure 3). The opposite effects of the dgk5 mutant and OE on plant growth under stress indicate that DGK5 suppresses Arabidopsis response to water and salinity stress and plays a negative role in plant growth under the abiotic stress conditions

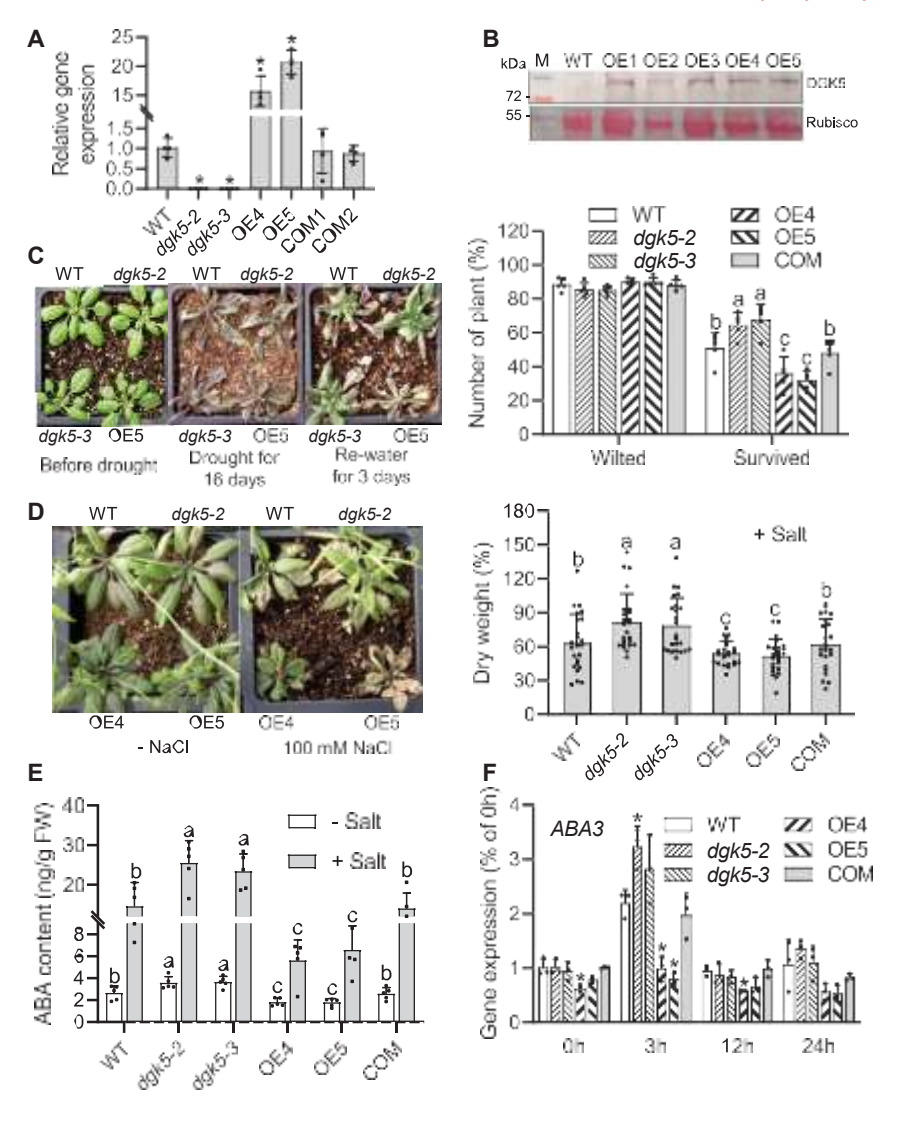


Figure 1. DGK5 negatively modulates plant growth under water and salt stress and inhibits ABA production.

- (A) Transcript levels of *DGK5* in WT, the *dgk5* mutants, OEs, and COM *Arabidopsis* expressed as fold changes to WT. Total RNA was extracted from 7-day-old seedlings as quantified by qPCR. Values are means  $\pm$  SD (n= 4 biological repeats). \*P < 0.05 compared with WT using Student's t-test.
- (B) Immunoblotting of YFP-Flag-DGK5 in WT and DGK5-OE Arabidopsis. Total proteins from 7-day-old plants were immunodetected using an anti-Flag antibody. Ponceau S staining of the large subunit of ribulose-bisphosphate carboxylase/oxygenase (Rubisco) on the membrane was used as a loading control. M, protein ladder.
- (C) Phenotype of WT, the *dgk5* mutant, and *DGK5*-OE *Arabidopsis* under drought. Two-week-old plants were subject to drought by withholding water for 16 days and then rewatered. Plant images were taken 16 days after drought and 3 days after rewatering and scored for wilted and survival plant rate, respectively, as shown in the right panel as percent of total plants tested. Values are means  $\pm$  SD (n = 5).
- (D) Phenotype of WT, the dgk5 mutant, and DGK5-OE Arabidopsis under NaCl stress. Three-week-old plants were subject to salt stress by watering without (control) or with 100 mM NaCl for 14 days. Plant images were taken 14 days after the treatment, and the above-ground tissues were collected for dry weight. The relative dry weight, as shown in the right panel, was calculated by comparing the values of NaCl-treated vs. control plants. Values are means  $\pm$  SD (n = 24). Different letters indicate statistical differences at P < 0.05 among genotypes under the same condition by one-way ANOVA.
- (E) ABA contents in WT and DGK5-altered Arabidopsis plants. After 3-week-old Arabidopsis plants were watered with or without 100 mM NaCl for 5 days, leaves were used for ABA measurements. Values are mean  $\pm$  SD (n = 4).

(F) Relative transcript levels of *ABA3* in WT and *DGK5*-altered *Arabidopsis* in response to NaCl. Three-day-old seedlings were transferred onto  $^{1}/_{2}$  MS medium plates and 14 days later the seedlings were treated with 100 mM NaCl. Total RNA was extracted and analyzed using qPCR. Values expressed as fold changes to WT at 0 h are mean  $\pm$  SD (n= 3 biological repeats). \*P< 0.05 compared with WT using Student's t-test.

### DGK5 suppresses ABA production

ABA is a plant hormone produced under stress and plays an important role in mediating plant response to various stressors, such as water and salinity. So, we measured ABA levels in WT and DGK5-altered Arabidopsis. Without applied stress, the ABA level was 30% higher in the dgk5 mutant plants, but 33% lower in DGK5-OE plants than WT (Figure 1E). The ABA levels increased greatly after plants were exposed to stress, but the magnitude of increase was in the order of the dgk5 mutant > WT > OE. At 100 mM NaCl, the ABA level increased about five-fold in WT, six-fold in the dgk5 mutant plants, and four-fold in OE plants. The ABA level in the dgk5 mutant plants was about two-fold higher than WT, whereas WT had more than two-fold higher ABA than DGK5-OE plants (Figure 1E). In addition, we measured ABA levels in young seedlings with and without salt treatments for 0, 0.5, 3, and 6 h. Consistent with the ABA changes in leaves, ABA levels increased in all genotypes after NaCl treatments for 0.5, 3, and 6 h, but the

magnitude of increase was the *dgk5* mutant > WT > OE (supplemental Figure 4, upper panel). The results indicate that DGK5 suppresses ABA production, particularly under stress.

We then examined the effect of *DGK5* alterations on the expression of genes involved in ABA biosynthesis (Figure 1F; supplemental Figure 5A). A previous study reported that the loss of DGK5 resulted in up- or down-expression of hundreds of genes (Kalachova et al., 2022), so we focused on a few genes directly involved in ABA synthesis. The expression of *DGK5* itself in WT was slightly increased 3 h after NaCl treatments (supplemental Figure 5A). Among the three genes in ABA biosynthesis tested, the transcript level of *ABA2* was irresponsive to salt stress, which was consistent with previous data (Gonza' lez-Guzma' n et al., 2002). By comparison, the transcript level of *ABA3* and *NCED3* (encoding 9-cisepoxycarotenoid dioxygenase 3) increased in response to salt stress in WT (Figure 1F; supplemental Figure 5A). The transcript

increase of *ABA3* was transient with the highest level at 3 h, whereas that of *NCED3* was sustained over 24 h (Figure 1F; supplemental Figure 5A). The transcript level of *ABA3* and *NCED3* increased more in the *dgk5* mutant plants, but less in *DGK5*-OE plants compared with WT (Figure 1F; supplemental Figure 5A). In particular, the *ABA3* transcript displayed almost no salt-induced increase in *DGK5*-OE (Figure 1F). Genetic complementation of the *dgk5* mutant plants restored the gene expression of the mutant to that of WT (Figure 1F; supplemental Figure 5A), verifying that the loss of *DGK5* is responsible for the altered gene expression in the *dgk5* mutants. The opposite changes in the expression of genes in ABA biosynthesis support that DGK5 suppresses stress-induced ABA production.

In addition, to test the effect of *DGK5* alterations on ABA-related physiological processes, we compared the water loss and stomatal aperture of DGK5-altered and WT leaves. DGK5-OE leaves lost more, whereas the dqk5 mutant plants lost less water than WT (supplemental Figure 5B). Without applied ABA, the stomatal aperture was similar among DGK5-altered and WT leaves (supplemental Figure 5C). After ABA treatments, the stomatal aperture of the dgk5 mutant plants was 30% smaller, whereas that of DGK5-OE was 15% larger than that of WT (supplemental Figure 5C). Genetic complementation of the dgk5 mutant plants restored the mutant response to that of WT (supplemental Figure 5B and 5C), supporting that the loss of DGK5 is responsible for the altered water loss and root growth phenotypes. The opposite effects on water loss and wider stomatal aperture by the dgk5 mutant and OE are consistent with the increased and decreased ABA levels in the dgk5 mutant and OE plants, respectively.

# DGK5 interacts with the ABA-synthesizing enzyme ABA2

To probe how DGK5 affects ABA levels and stress responses, we performed a database search and came across a report indicating potential DGK5 and ABA2 binding from a proteome-wide yeast two-hybrid protein-protein interaction mapping study of Arabidopsis (Arabidopsis Interactome Mapping Consortium, 2011). ABA2 (At1g52340) catalyzes the conversion of xanthoxin to abscisic aldehyde in ABA synthesis, and the loss of ABA2 decreased ABA production and rendered plants lose more water (Gonza' lez-Guzma' n et al., 2002). Therefore, we tested whether DGK5 interacts physically with ABA2 using complementary approaches (Figure 2). GST-tagged DGK5 and His-tagged ABA2 were expressed in E. coli and purified to apparent homogeneity. Glutathione-agarose beads pulled down GST and GST-DGK5, as expected, and GST-DGK5bound beads also co-pulled down His-ABA2 (Figure 2A). However, mixing His-ABA2 with GST only did not pull down ABA2 (Figure 2A), suggesting that DGK5 was responsible for the coprecipitation of ABA2.

In addition, to verify the protein–protein interaction, we coexpressed DGK5 and ABA2 in tobacco leaves by co-infiltrating leaves with p35S::ABA2-HA-CFP and p35S::DGK5-YFP-Flag or the control p35S::YFP-Flag without DGK5. Leaf proteins were precipitated with an anti-HA antibody, followed by immunoblotting with an anti-Flag antibody (Figure 2B). DGK5-YFP-Flag, but not YFP-Flag, was detected in the immunoprecipitants (Figure 2B), indicating that DGK5 and ABA2 expressed in plant leaves are co-precipitated. These results from plant- and *E. coli*-expressed proteins indicate that DGK5 physically interacts with ABA2.

Furthermore, we used bimolecular fluorescence complementation (BiFC) to test the DGK5 and ABA2 interaction in Arabidopsis cells (Figure 2C). ABA2 and DGK5 were fused to the N-terminal (NY-ABA2) and the C-terminal (CY-DGK5) fragments of YFP, respectively. In addition, we fused a nuclear marker histone H2B with mCherry (mCherry-H2B) as a control for the transfection and nuclear localization, and we also fused DGK1 to the C-terminal fragment (CY-DGK1) of YFP as a control for the interaction specificity (Figure 2C). Co-transfection of NY-ABA2 and CY-DGK5 into Arabidopsis protoplasts led to YFP fluorescence in the nuclei and cytoplasm (Figure 2C, far right panels). However, no YFP fluorescence was observed in protoplasts co-transfected with NY-ABA2 and CY or NY and CY-DGK5 (Figure 2C, left two panels). Likewise, cotransfection of NY-ABA2 and CY-DGK1 resulted in no detection of YFP fluorescence (Figure 2C, third panels), suggesting that ABA2 does not interact with DGK1. All introduced constructs were expressed as the transcripts were detected using semi-quantitative PCR (Figure 2D). Moreover, we performed ABA2 protein truncations to map the region of ABA2 involved in DGK5 binding (supplemental Figure 6). Deletion of the N-terminal 32 amino acid fragment (F1) led to the loss of BiFC with DGK5, whereas ABA2 C-terminal truncations of 75 amino acids (R1) and 122 amino acids (R2) fragments still exhibited BiFC with DGK5 as did the full-length ABA2 (supplemental Figure 6C). Those results indicate that DGK5 and ABA2 interact and that the N-terminal 32 amino acids region of ABA2 is involved in binding DGK5.

# Loss of DGK5 function decreases nuclear association of ABA2

The above results suggest that DGK5 is associated with nuclei, with some being in the cytoplasm and the plasma membrane. To verify the subcellular distribution, we introduced 35S::YFP-Flag-DGK5 into tobacco leaves and found the YFP signal in nuclei and cell periphery outside the nucleus in leaves (Figure 3A). Meanwhile, we generated Arabidopsis plants expressing 35S::YFP-Flag-DGK5, which also showed the YFP signal in nuclei and outside the nucleus in root cells (Figure 3B). To validate the nuclear association, we performed subcellular fractionation by isolating the nuclear and cytosolic fractions from plants harboring the 35S::YFP-Flag-DGK5, followed by immunoblotting. Successful fractionation was verified by detecting the nuclear marker histone H3 proteins and the cytosolic marker phosphoenolpyruvate carboxylase 1 (PEPC1) (Figure 3C). PEPC1 was detected in the cytosolic fraction (C) but absent in the nuclear pellet (N) while histone H3 was in the nuclei but not in the cytosolic fraction, indicating that those two fractions were well separated with no apparent cross-contamination (Figure 3C). The DGK5 band was detected in both the nuclear and cytosolic fractions (Figure 3C). Those results support the imaging data that DGK5 is associated with nuclei and present extranuclearly.

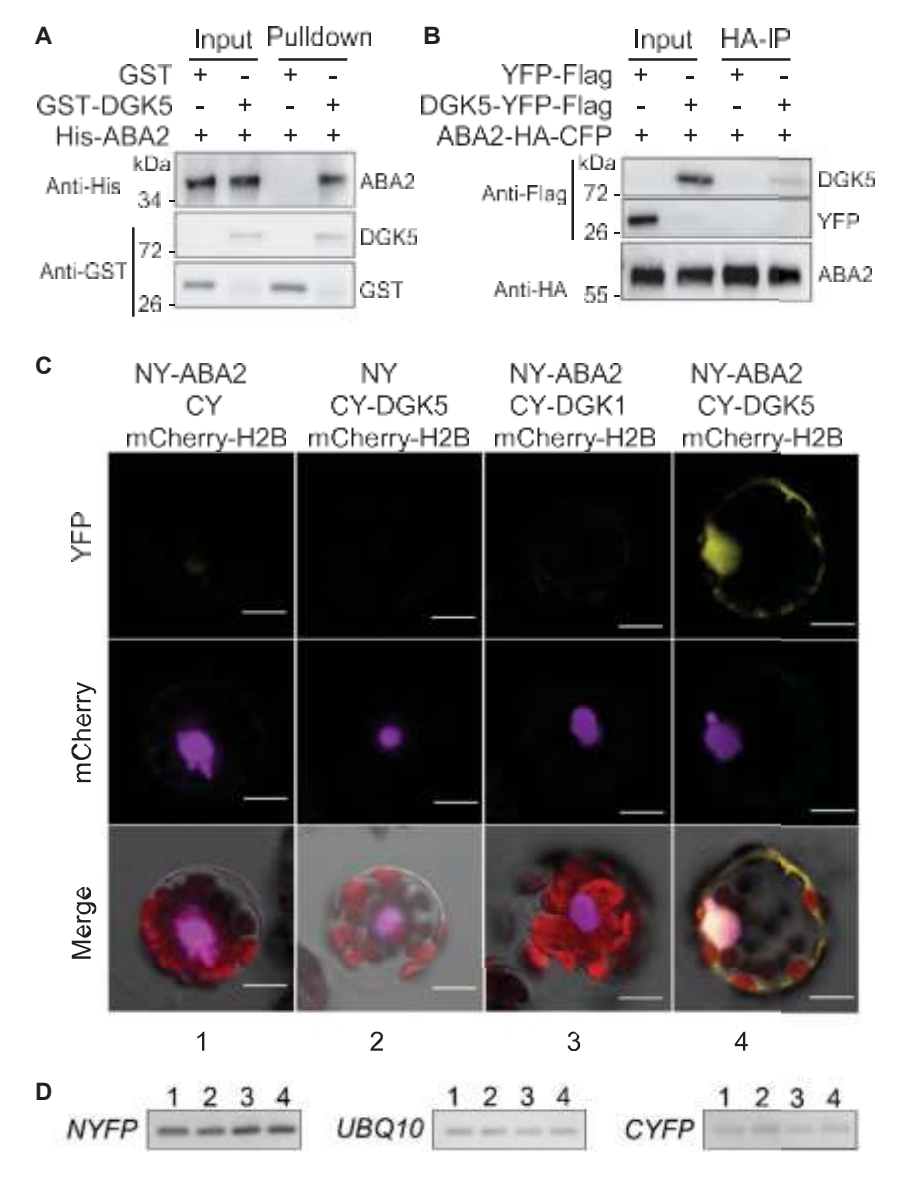


### Figure 2. DGK5 interacts with ABA2.

- (A) Immunoblotting of ABA2 co-pulled down with GST-DGK5. His-ABA2 proteins pulled down by GST-DGK5-immobilized beads were immunodetected using an anti-His antibody, and GST or GST-DGK5 proteins were immunodetected using an anti-GST antibody.
- (B) Coimmunoprecipitation of DGK5 and ABA2 in tobacco leaves. Total proteins were extracted from the tobacco leaves expressing p35S::ABA2-HA-CFP/p35S::YFP-Flag or p35S::ABA2-HA-CFP/p35S::DGK5-YFP-Flag. Immunoprecipitation (IP) was performed using an anti-HA antibody and protein A agarose, and then immunodetections of ABA2 and DGK5 were performed using the antibodies indicated on the left.
- (C) BiFC imaging of DGK5-ABA2 interaction in *Arabidopsis* protoplasts. The plasmid combinations nYFP-ABA2/cYFP, nYFP/cYFP-DGK5, nYFP-ABA2/cYFP-DGK1, and nYFP-ABA2/cYFP-DGK5 were transfected into *Arabidopsis* protoplasts. mCherry-H2B was co-transfected as the positive transfection control and a nuclear marker. Protoplasts transformed with nYFP-ABA2/cYFP-DGK5 showed the fluorescent signal in the nucleus and cytosol, whereas no fluorescent signal was observed in the protoplasts transformed with other plasmid combinations. Scale bars correspond to 10 mm.
- (D) Transcript levels of *ABA2*, *DGK1*, and *DGK5* in the protoplasts from (C). Total RNA was extracted from the protoplasts transformed with NY-ABA2/CY (1), NY/CY-DGK5 (2), NY-ABA2/CY-DGK1 (3), or NY-ABA2/CY-DGK5 (4). The expression levels of *ABA2*, *DGK1*, and *DGK5* were measured by semi-quantitative PCR with primers for the N-terminal region (NYFP) and C-terminal region (CYFP) of YFP, and normalized by ubiquitin 10 (*UBQ10*).

In addition, we examined the effect of DGK5 on the subcellular distribution of ABA2. CFP-fused ABA2 was transiently expressed in the dgk5 mutant, OE, and WT Arabidopsis leaves, followed by confocal imaging and subcellular fractionation. ABA2-CFP was mostly associated with the cytoplasm, with some ABA2-CFP being in nuclei (Figure 3D; supplemental Figure 7A). Compared with WT, more ABA2 was associated with the nuclei in DGK5-OE, but less in the dgk5 mutant based on the ratio of nuclear vs. cytosolic ABA2-CFP signals (Figure 3D). In addition, based on the percentage of nuclei with detectable ABA2, more ABA2 was present in the nuclei of DGK5-OE, but fewer in the nuclei of the dgk5 mutant (supplemental Figure 7A). The results verify that ABA2 is associated with cytoplasm and nuclei and, moreover, indicate that the presence of DGK5 enhances the nuclear association of ABA2. We further tested the effect of salt stress on ABA2 subcellular distribution by incubating the Arabidopsis leaves infiltrated with ABA2 with or without NaCl. Under NaCl stress, the nuclear ABA2 to cytosolic ABA2 ratio was slightly increased in WT. The ratio of nuclear ABA2 to cytosolic ABA2

tended to be lower in the *dgk5* mutant but higher in *DGK5*-OE plants with 100 mM NaCl for 2 h (Figure 3D).

# DGK5 activity and PA promote nuclear association of ABA2

To test whether DGK5 enzymatic activity is involved in promoting the nuclear association of ABA2, we generated an enzymatic activity-dead DGK5d by mutating G112, as described previously (Kalachova et al., 2022; Scholz et al., 2022). ABA2-CFP with the YFP empty vector, the DGK5d mutant, or with DGK5 was coexpressed in the *dgk5* mutant plants, followed by examining the ABA2's subcellular association. More nuclear ABA2-CFP was detected in the *dgk5* mutant co-expressed with active DGK than that with the DGK5d mutant that displayed a similar level of nuclear association of ABA2 as that co-expressed with the YFP empty vector control (Figure 3E; supplemental Figure 7B). The results indicate that DGK5 activity mediates the DGK5-promoted nuclear association of ABA2. We then tested the effect of PA on ABA2's nuclear association by supplying PA

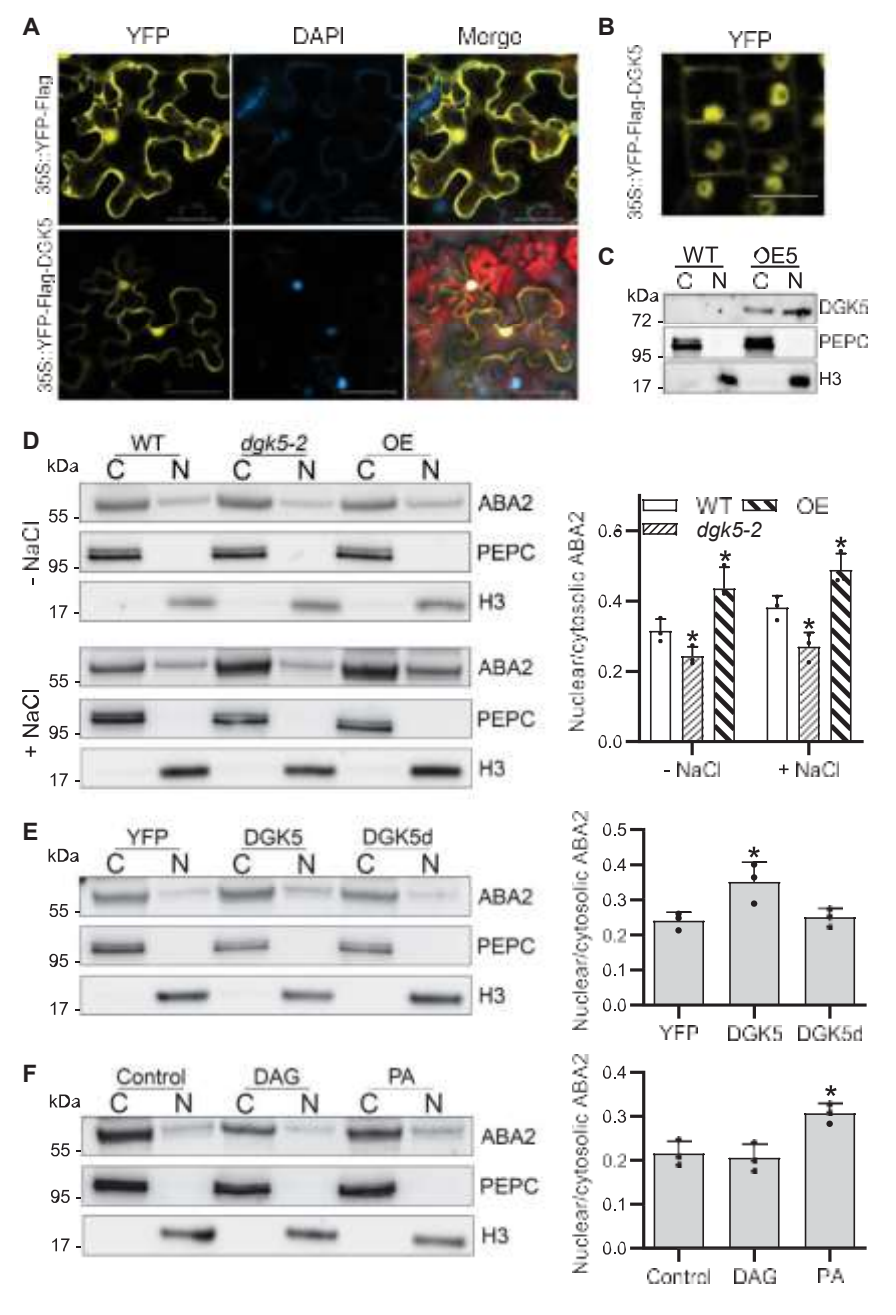


Figure 3. DGK5 and ABA2 are located in and outside the nuclei.

- (A) Confocal imaging of tobacco leaves transiently expressing p35S::YFP-Flag or p35S::YFP-Flag-DGK5. The tobacco leaves were infiltrated with the agrobacteria carrying p35S::YFP-Flag or p35::YFP-Flag-DGK5 and observed under a confocal microscope. The nuclei were stained with 4º,6-diamidino-2-phenylindole (DAPI). Scale bars correspond to 50 mm.
- (B) Confocal imaging of *Arabidopsis* root cells. Five-day-old *Arabidopsis* expressing *p35S::YFP-Flag-DGK5* was observed. Scale bar corresponds to 20 mm
- (C) Immunoblotting of YFP-Flag-DGK5 in nuclear and cytosolic fractions. Cytosolic and nuclear fractions were isolated from WT and YFP-Flag-DGK5 *Arabidopsis* seedlings. YFP-Flag-DGK5 was immunodetected using an anti-Flag antibody. Phosphoenolpyruvate carboxylase (PEPC) and histone H3 were used as a cytosolic (C) and a nuclear (N) marker, respectively.
- (D) Immunoblotting of ABA2-HA-CFP in cytosolic and nuclear fractions under NaCl stress. The quantification of nuclear ABA2 to cytosolic ABA2 ratio shown on the right was calculated based on ABA2 band intensity in nuclear and cytosolic fractions on the left as measured using ImageJ. Values are means  $\pm$  SD from three biological replicates. \*P < 0.05 compared with WT using Student's *t*-test.
- (E) Immunoblotting of ABA2-HA-CFP in cytosolic and nuclear fractions in the presence of enzymeactive DGK5 or enzyme-dead DGK5 (DGK5d). The quantification of the nuclear ABA2 to cytosolic ABA2 ratio is shown on the right. Values are means  $\pm$  SD from three biological replicates. \*P < 0.05 compared with YFP empty vector control using Student's t-t-est.
- (F) Immunoblotting of ABA2-HA-CFP in cytosolic and nuclear fractions in response to lipid treatment. The nuclear ABA2 to cytosolic ABA2 ratio was quantified on the right. Values are means  $\pm$  SD from three biological replicates. \*P < 0.05 compared with the solvent control using Student's t-test.

to leaves transformed with ABA2. PA increased the nuclear association of ABA2 compared with those without PA treatments (Figure 3F; supplemental Figure 7C). Those results further support that the DGK5 activity and its lipid product PA promote the nuclear association of ABA2.

# DGK5 and PA suppress ABA2 activity

To determine the function of DGK5–ABA2 interaction, we tested the effect of DGK5 and its lipid substrate DAG and product PA on ABA2 activity. Co-incubation of DGK5 and ABA2 proteins at the 1:1 M ratio lowered about 14% ABA2 dehydrogenation activity (Figure 4A). However, PA is much more effective in inhibiting ABA2 activity that was decreased by 75% in the presence of di-18:1-PA or egg yolk PA, but not in the presence of di-18:1-

DAG or egg yolk phosphatidylcholine (PC) (Figure 4B). Increased PA to ABA2 molar ratios increased ABA2 inhibition, and ABA2 activity was abolished at the 8:1 PA/ABA2 molar ratio, but DAG showed no inhibition of ABA2 activity at all the ratios tested (Figure 4C). The presence of PA in the reaction decreased apparent  $V_{\rm max}$  (14.7 vs. 9.7 mM NADH/min with PA) toward the substrate, but did not change the apparent  $K_{\rm m}$ , (0.156 vs. 0.152 mM with PA), indicating that the PA is a noncompetitive inhibitor of ABA2 (Figure 4D).

We then tested the common phospholipid constituents of the cell membranes to see whether ABA2 specifically bound PA using two complementary approaches. ABA2 bound PA, but not other anionic lipids tested, such as phosphatidylinositol (PI), phosphatidylinositol-4-phosphate [PI(4)P), phosphatidylinositol

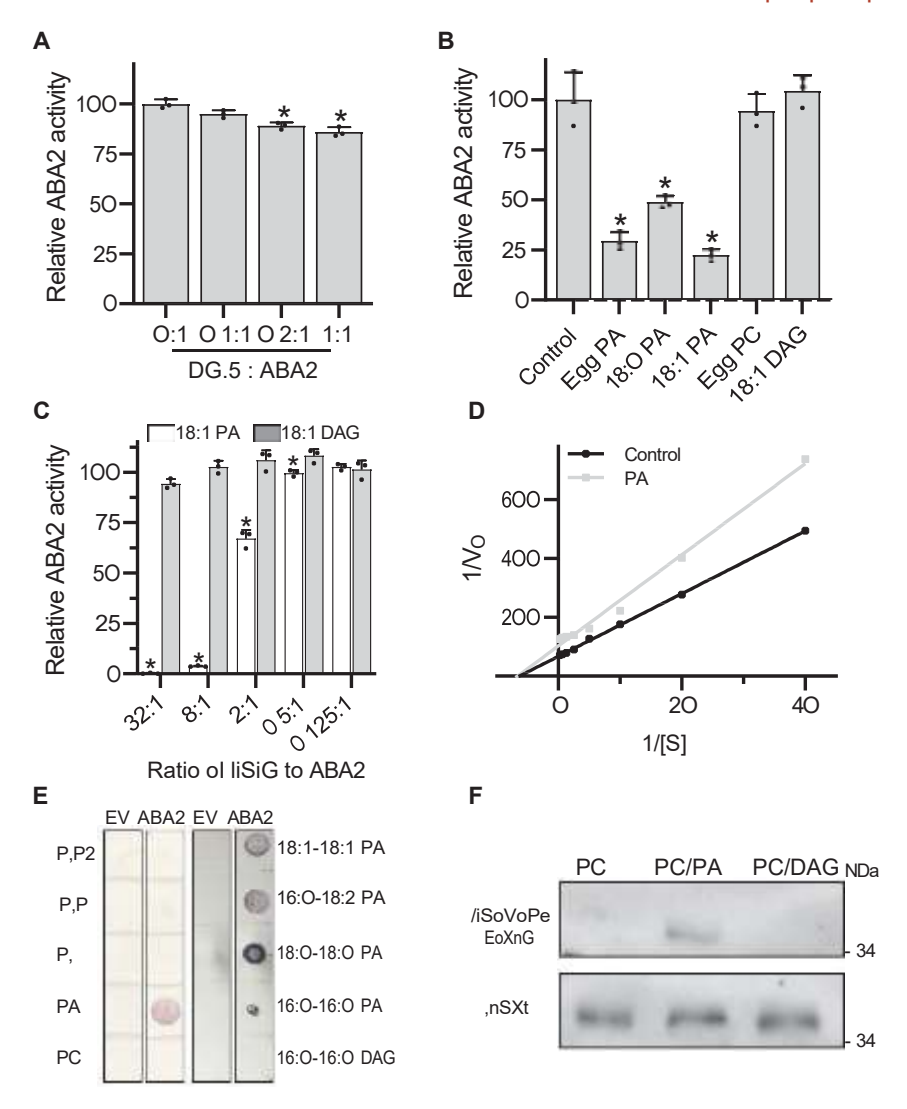


Figure 4. PA binds ABA2 and inhibits its activity.

- (A) DGK5's effect on ABA2 activity assayed in the absence or presence of DGK5 with the fixed amount of ABA2. Values are means  $\pm$  SD (n = 3) expressed as relative values to ABA2 activity in the absence of DGK5. \*P < 0.05 compared with ABA2 activity in the absence of DGK5 using Student's t-test.
- (B) Lipid effect on ABA2 activity assayed in the absence or presence of different lipids (2 mg). Values are means  $\pm$  SD (n= 3) expressed as relative values to the solvent control. \*P < 0.05 compared with control using Student's t-test. PA, phosphatidic acid; PC, phosphatidylcholine; DAG, diacylglycerol. (C) PA inhibition of ABA2 activity assayed in the presence of increased amounts of PA or DAG in molar ratios. Values are means  $\pm$  SD (n= 3) shown as relative values to ABA2 activity in the absence of lipids. \*P < 0.05 compared with ABA2 activity in the absence of lipids by Student's t-test.
- (D) Double-reciprocal plot of ABA2 activity in the absence or presence of di-18:1 PA at 5:1 PA:ABA2 ratio.
- (E) Filter-blotting of ABA2 binding to PA. Lipids (5 mg) spotted on a nitrocellulose membrane, which was then incubated with purified empty vector (EV) or His-ABA2 (1.5 mg/ml). His-ABA2 was immunodetected using an anti-His antibody. The left two blots show mixed molecular species of PA and PC from egg yolk, PI (phosphatidylinositol) from soybean, 17:0-20:4 PI(4)P, and 16:0-16:0 PI(4,5)P2; The right two blots show specific molecular species of PA or DAG (F) Liposome pull down of ABA2. Purified His-ABA2 was incubated with liposomes made of di-18:1-PC/ di-18:1-PA (3:1), di-18:1-PC/di-18:1-DAG (3:1), or di-18:1-PC only and pulled down by centrifugation. Liposome-associated ABA2 was immunoblotted using an anti-His antibody. "Input" represents the samples prior to centrifugation.

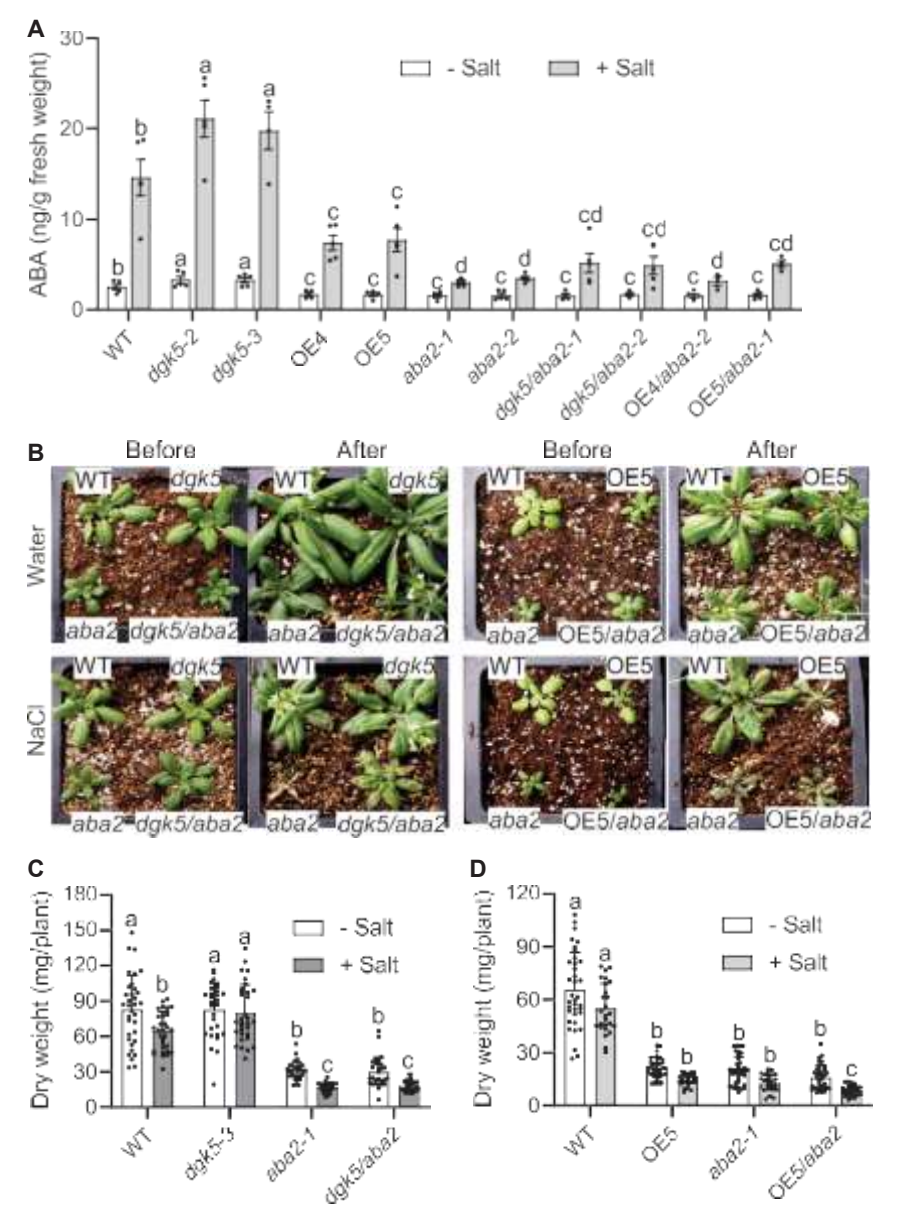
(4,5)-bisphosphate (PI(4,5)P<sub>2</sub>] or phosphatidylglycerol (PG), or other phospholipids, including phosphatidylserine (PS) or PC based on filter binding (Figure 4E, left panel; supplemental Figure 6D). ABA2 bound various PA species tested, including di-18:1-PA, 16:0/18:2-PA, di-18:0-PA, and di-16:0-PA, but not di-16:0-DAG (Figure 4E, right panel). With liposomal binding, ABA2 was pulled down with PC liposomes containing PA, but not those containing DAG or PC only (Figure 4F). PC was used as a carrier lipid because PA alone does not form liposomes. Those results indicate that PA binds to ABA2 and inhibits its enzyme activity.

### DGK5 acts through ABA2 to affect ABA production

To test the interaction of DGK5 and ABA2 further, we obtained two aba2 mutants, verified the loss of the ABA2 transcript in the mutants (supplemental Figure 8A–8C), and then crossed them with the dgk5 mutant to generate plants null in both DGK5 and ABA2. Without applied stress, the aba2 mutant and DGK5-OE plants had similar ABA levels, which were lower than WT in leaves of soil-grown plants (Figure 5A) or seedlings on plates (supplemental Figure 4, upper panel). Under NaCl stress, ABA levels were induced in WT and the dgk5 mutant, but the

magnitude of induction was subdued in *DGK5*-OE, the *aba2* mutants, and double mutants, *dgk5xaba2* or *DGK5*-OExaba2 (Figure 5A; supplemental Figure 4, upper panel). Similarly, the NaCl-induced ABA increases in the *dgk5* mutant plants were lost in the *dgk5/aba2* double mutants (*dgk5-2/aba2-1*, *dgk5-2/aba2-2*, *DGK5-OE/aba2-1*, or *DGK5-OExaba2-2*) (Figure 5A; supplemental Figure 4, upper panel). Thus, while the *dgk5* mutant and OE had a higher and lower level, respectively, of ABA content than WT plants, there was no significant difference in ABA contents among the *dgk5* mutant or OE plants when ABA2 was disrupted, either without or with NaCl stress (Figure 5A; supplemental Figure 4, upper panel). Those results suggest that ABA2 is required for the DGK5 effect on ABA production.

In addition, we measured the effect of those *DGK5* and *ABA2* mutations on plant growth under NaCl stress (Figure 5B–5D; supplemental Figure 8D and 8E). Compared with WT, the *dgk5* mutant plants grew bigger, whereas the *aba2* mutant and *dgk5xaba2* grew smaller. In contrast, *DGK5*-OE plants grew smaller like *aba2*, whereas the *DGK5*-OExaba2 double mutant was further smaller (Figure 5B – 5D; supplemental Figure 8D and 8E). The biomass results were consistent with the ABA measurements, and the loss of *ABA2* abolished the effect of the



dgk5 mutant and OE, suggesting that DGK5 acts mostly epistatic to ABA2 in terms of ABA production and plant growth in response to stress.

### DGK5 increases cellular PA/DAG ratio

As DGK phosphorylates DAG to produce PA, we compared DAG and PA levels in WT and *DGK5*-altered *Arabidopsis* lines to assess the effect of *DGK5* alterations on the lipid substrate and product (Figure 6). We used roots first for the analysis because DGK5 is highly expressed in roots and additionally roots are low in galactolipids that predominate in green tissues. Without applied stress, the total cellular level of PA was similar between WT and the *dgk5* mutants (*dgk5-2* and *dgk5-3*), but *DGK5-OE* had a 40% higher PA than other genotypes (Figure 6A). However, under NaCI stress, the PA level was 22% lower in the *dgk5* mutants but 25% higher in *DGK5-OE* than WT (Figure 6A). The *aba2* mutants (*aba2-1* and *aba2-2*) and WT had similar levels

# Figure 5. ABA contents and growth of *dgk5* and *aba2* mutants under salt stress.

(A) ABA contents in WT and *DGK5/ABA2* single and double mutants without and with salt stress. ABA was measured from leaves of 3-week-old *Arabidopsis* plants watered with or without 100 mM NaCl for 5 days. Values are mean ± SD (*n* = 5).

(B) Phenotypes of *DGK5* and *ABA2* mutants without and with salt stress. Three-week-old *Arabidopsis* plants were subject to salt stress by watering without (water) or with 100 mM NaCl (NaCl) for 5 days. The images were taken immediately before salt (before) and 5 days after salt stress (after), respectively.

(C and D) Dry weights of *DGK5* and *ABA2* mutants without and with salt stress. The above-ground tissues of plants shown in (B) were collected for dry weights. Values are mean  $\pm$  SD (n = 30 seedlings with 5 biological repeats). Different letters indicate statistical differences at P < 0.05 among genotypes under the same condition by one-way ANOVA.

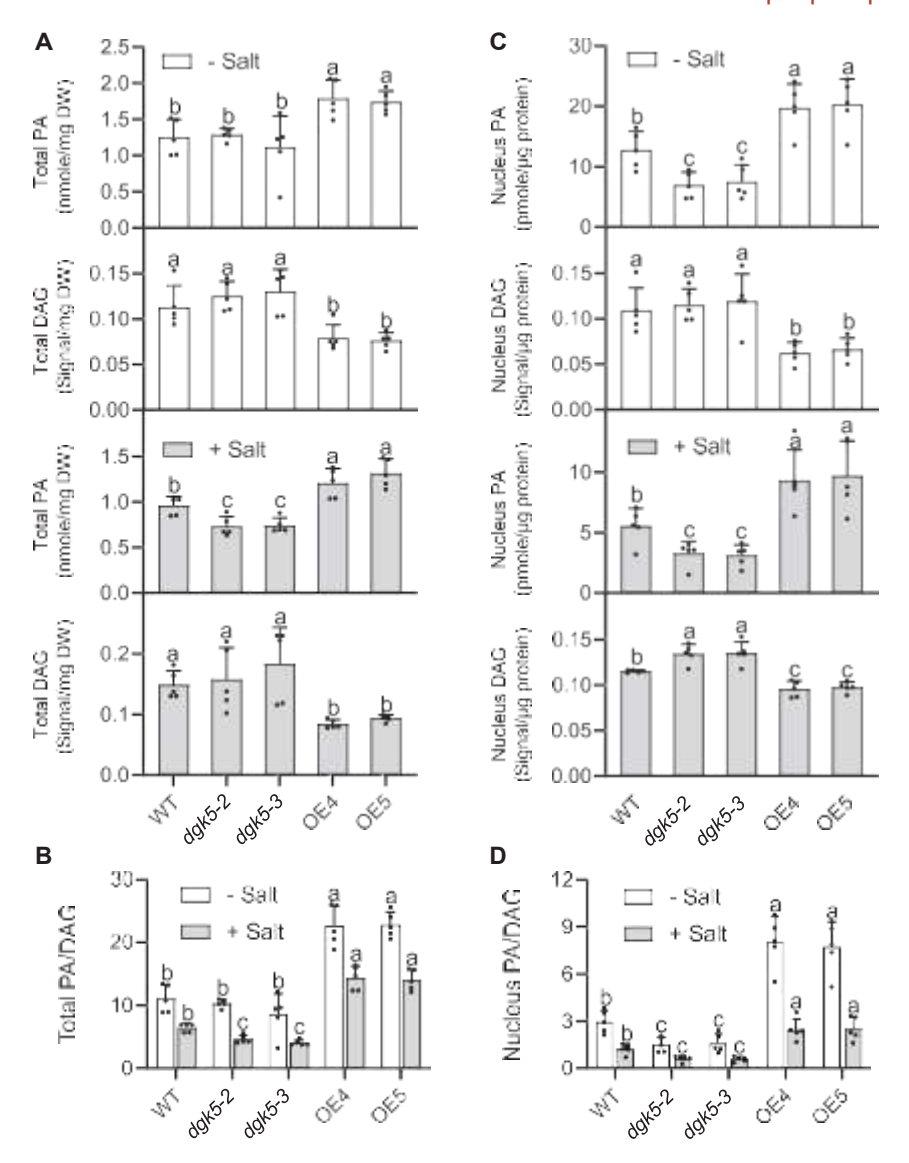
of PA, whereas *dgk5xaba2* and *DGK5-OExaba2* displayed lower and higher PA levels, respectively, like the effect of *dgk5* and *DGK5-OE* single mutants (supplemental Figure 9A). The results suggest that ABA2 does not impact the effect of DGK5 on PA formation. The opposite changes of PA in the *dgk5* mutant and OE plants indicate a role of DGK5 in producing cellular PA.

The DAG level in *DGK5*-OE plants displayed opposite changes as PA in the mutants (Figure 6A). DAG was 10%–16% lower in *DGK5*-OE and *DGK-OExaba2* than WT without applied stress, and the decrease grew to 43% under NaCl stress (Figure 6A). The DAG level in the *dgk5* mutants was significantly different from that of WT. The *aba2* mutants (*aba2-1* and *aba2-2*), *dgk5xaba2*, and WT had similar levels of

DAG, whereas *DGK5-OExaba2* displayed a lower DAG level, like the effect of *DGK5-OE* single mutants (supplemental Figure 9A). The results suggest that ABA2 does not impact the effect of DGK5 in cellular DAG level with or without NaCl stress. To help better visualize the effect of DGK5 on the lipid changes, we compared the PA-to-DAG ratios between *DGK5*-altered and WT plants (Figure 6B). The PA/DAG ratio was lower in the *dgk5* mutants, but higher in *DGK5-OE* than that of WT. *ABA2* mutants and WT had a similar PA/DAG ratio, whereas *dgk5xaba2* and *DGK5-OExaba2* displayed a lower and higher PA/DAG ratio, respectively, like the effect of *dgk5* and *DGK5-OE* single mutants (supplemental Figure 9B).

DGK5 affects nuclear PA/DAG ratio more than total cellular lipids

Since DGK5 was associated mostly with nuclei, we analyzed PA and DAG levels in nuclei (Figure 6C). Nuclei were isolated from



Arabidopsis seedlings in the presence of an elevated level of the cation chelator EGTA in all buffers to suppress lipolytic activity (Kim et al., 2019), followed by lipid analysis of the nuclear fraction. The nuclear fraction without apparent cytosolic contamination was verified by detecting histone H3 proteins and PEPC1, respectively, as in Figure 3C and 3D. The nuclear PA level was about 40% lower in the dgk5 mutants but was 45% higher in DGK5-OE than that in WT with or without NaCl stress (Figure 6C). The lower PA in the dgk5 mutants without applied stress is unlike the total cellular PA, which displayed no apparent decrease in the dgk5 mutants without stress. The aba2 mutants and WT were similar in nuclear PA levels, and dgk5xaba2 and DGK5-OExaba2 displayed a lower and higher PA level, respectively, like the effect of dgk5 and DGK5-OE single mutants (supplemental Figure 9C), suggesting that ABA2 does not influence the effect of DGK5 on nuclear PA levels. Those results suggest that DGK5 contributes to the nuclear PA accumulation.

The nuclear DAG level was similar between WT and the *dgk5* mutants, including *dgk5xaba2* in normal condition, but it was higher

# Figure 6. *DGK5*changes nuclear PA and DAG levels

- (A) Total PA and DAG levels in WT and the dgk5 mutant and OE roots without and with salt stress.(B) Total PA/DAG ratios in WT and the dgk5 mutant and OE roots without and with salt stress.
- (C) Nuclear PA and DAG levels in WT and the *dgk5* mutant and OE roots without and with salt stress.
  (D) Nuclear PA/DAG ratios in WT and the *dgk5* mutant and *DGK5*-OE roots without and with salt stress. Total PA levels were calculated as nmole per
- mutant and *DGK5*-OE roots without and with salt stress. Total PA levels were calculated as nmole per mg dry weight, whereas nuclear PA was expressed as pmole per mg protein. Total DAG levels are expressed as relative mass spectral signal per mg dry weight, whereas nuclear DAG is expressed as relative mass spectral signal per mg protein. Different letters indicate differences at *P* < 0.05 among genotypes under the same conditions by one-way ANOVA.

in the dgk5 mutants than WT with NaCl stress. In contrast, the nuclear DAG level in DGK5-OEs was substantially lower than WT with or without NaCl stress (Figure 6C). When the nuclear PA/DAG ratios were compared, the dgk5 mutants had a lower, whereas DGK5-OEs including DGK5-OExaba2 had a higher PA/DAG ratio than WT with salt stress (Figure 6D). Without salt stress, the total PA/ DAG ratios were similar in WT and the dgk5 mutant, but higher in OE, supporting that overexpressing DGK5 produced more PA than WT and the dgk5 mutant. With salt stress, the total PA/DAG ratio in WT was higher than that in the dgk5 mutant, but lower than that in OE. The data support that WT with salt-increased DGK5 produced more PA than the dgk5 mutants. In addition, while DGK5-OE produced more PA than WT with or without salt, the percent increase of PA/ DAG under NaCl relative to unstressed plants

in *DGK5*-OE was lower than the percent increase in WT. This could result from the possibility that DGK5 is NaCl induced in WT, whereas the DGK activity in OE plants came mostly from the constitutive 35S-driven *DGK5*. Thus, the difference between WT and the *dgk5* mutant is more informative to the native DGK5 effect. The magnitude of the nuclear PA/DAG differences between WT and *DGK5*-altered nuclei was greater than the total PA/DAG in roots. The results suggest that DGK5 acts in nuclei, consistent with its association with nuclei.

In WT *Arabidopsis* roots, the most abundant molecular species of DAG were 18:3/16:0-, 18:2/16:0-, and 18:3/18:2-DAG, followed by 18:2/18:2- and 18:3/18:3-DAG species (supplemental Figures 10 and 11). Most major DAG species increased in the *dgk5* mutant but decreased in *DGK5*-OE roots with or without stress (supplemental Figures 10 and 11). Conversely, the major molecular species of PA, such as 34:2-, 34:3-, 36:5-, 36:4-, and 34:6-PA, were all decreased in the *dgk5* mutant but increased in *DGK5*-OE roots (supplemental Figures 12 and 13). The direction of DAG and PA changes in *DGK5*-OE and the *dgk5* mutant plants

are consistent with the role of DGK5's conversion of DAG to PA. Comparing DAG species from nuclear and total lipid extracts, 18:3/16:0- and 18:2/16:0-DAGs were the most common DAG species, but 18:3/18:2- and 16:0/16:0-DAGs, together with 18:3/16:0- and 18:2/16:0-DAGs, become abundant in the WT nuclear fraction (supplemental Figures 10 and 11). Only a few nuclear DAG species displayed increases in the *dgk5* mutant but decreases in OE (supplemental Figures 10 and 11). The major PA species, 34:2-, 34:3-, 36:5-, and 36:4-PAs (supplemental Figures 12 and 13), were like those of total PA in seedling roots (supplemental Figures 12 and 13). The nuclear fraction exhibited significantly less accumulation of the major species of PA in the *dgk5* mutants, but more in *DGK5*-OE lines (supplemental Figures 12 and 13). These results suggest that the *DGK5* alterations affect the DAG/PA homeostasis in *Arabidopsis*.

### Salt stress induced a transient increase in PA

We further examined the time-dependent PA changes using WT and DGK5-altered seedlings treated with 100 mM NaCl for 0, 0.5, 5, and 6 h. PA increased transiently at 0.5 h and then decreased at 3 and 6 h (supplemental Figure 4). Without applied stress, the total PA level was not significantly different between WT and the dgk5 mutants (dgk5-3 or dgk5/aba2) or aba2 seedlings, but DGK5-OE (OE5 or OE5/aba2) had a higher PA level than other genotypes (supplemental Figure 4, second panel, 0 h). Conversely, the DAG level was lower in DGK5-OE plants than WT, the dgk5, and aba2 mutants (supplemental Figure 4, third panel, 0 h). However, after NaCl treatments, the dgk5 mutants (dgk5-3 or dgk5/aba2) had a lower PA level than WT and aba2 seedlings, but DGK5-OE (OE5 or OE5/aba2) mutants had a higher PA level (supplemental Figure 4, second panel, 0.5, 3, and 6 h). By comparison, the DAG level was lower in DGK5-OE plants than WT and the dgk5 mutant seedlings (supplemental Figure 4, third panel, 0.5, 3, and 6 h). The PA/ DAG ratio was lower in the dgk5 mutant, but higher in DGK5-OE than that of WT with salt stress (supplemental Figure 4, bottom panel, 0.5, 3, and 6 h).

WT and aba2 had a similar PA/DAG ratio, whereas dgk5/aba2 and DGK5-OExaba2 displayed a lower and higher PA/DAG ratio, respectively, similar to dgk5 and DGK5-OE single mutants (supplemental Figure 4, bottom panel, 0.5, 3, and 6 h). Without salt stress, the PA/DAG ratio was not significantly different between WT and the dgk5 mutant, but higher in OE, supporting that overexpressing DGK5 produced more PA than WT and the dgk5 mutant. With salt stress, the PA/DAG ratio in WT was higher than that in the dgk5 mutant, but lower than that in OE. The data support that WT that contains the salt-increased DGK5 produced more PA than the dak5 mutant. Like the 10-h NaCl treatment, the percent salt-induced PA/DAG increase relative to un-stressed in DGK5-OE seedlings was lower than the percent increase in WT, which might be because DGk5 was increased under salt in WT but the DGK activity in OE plants came mostly from the constitutive 35S-driven DGK5.

## DISCUSSION

Lipid phosphorylation by DGKs plays important roles in various plant processes, but the mechanism of action remains mostly unknown. This study shows that DGK5 suppresses the biosynthesis

of ABA, which is a major stress-induced hormone to help plant adaptation to abiotic challenges, such as drought, salt, and osmotic stress conditions. Specifically, the data document that DGK5 and PA bind to the ABA biosynthesizing enzyme ABA2 and inhibit its activity. ABA measurements provide further support for the negative role of DGK5 in ABA accumulation as ABA levels were decreased in *DGK5*-OE and increased in the *dgk5* mutant plants. Therefore, this study identifies a novel mechanism of DGK5 action; DGK5 interacts directly with ABA2, and the lipid product PA attenuates ABA2 activity to suppress stress-induced ABA production (Figure 7).

The DGK5 suppression of ABA production is consistent with its negative effect on plant response to abjotic stressors, such as water deficits and salinity. DGK5-OE, which is decreased in ABA levels, showed increased stress damage, whereas the dgk5 mutant plants with increased ABA levels displayed decreased stress damage to water and salt stress. The dgk5 mutant Arabidopsis plants were also reported to exhibit enhanced freezing tolerance (Tan et al., 2018). A recent study reported that the loss of DGK5 increased Arabidopsis susceptibility to Pseudomonas syringae, suggesting a positive role of DGK5 in bacterial infection (Kalachova et al., 2022). The role of ABA in plant-pathogen interactions varies, depending on infection phases and pathogen types. ABA mainly plays a negative role in post-invasive defense, such as inhibiting callose deposition and pathogen-associated molecular pattern-induced gene expression elicited by the bacterial pathogen P. syringae pv. tomato (de Torres-Zabala et al., 2007). So, the increased sensitivity of the dgk5 mutant to the pathogen is consistent with higher ABA levels resulting from the DGK5 and PA inhibition of ABA production.

The subcellular associations of DGK5 and ABA2 provide further insights into the function of the DGK5-ABA2 interaction. This study shows that DGK5 and ABA2 are associated with nuclei and extranuclearly, but their relative distribution differs. Such subcellular distribution of DGK5 and ABA2 is consistent with other observations (Cheng et al., 2002; Kalachova et al., 2022; Li et al., 2022). The majority of ABA2 is localized in the cytoplasm, and so is the ABA2-catalyzed reaction in ABA synthesis. However, the current results indicate that DGK5 and PA promote ABA2's nuclear association. Our lipid analysis supports that DGK5 functions in nuclei because the dgk5 mutant decreased, whereas DGK5-OE increased the nuclear PA/DAG ratio compared with WT, and the PA/DAG differences are greater in nuclear lipids than total lipids. These changes are consistent with the role of DGK5 that converts DAG to PA in nuclei. This was also consistent with the data that nuclear DGKs regulate the levels of DAG in the nucleus in animals and yeast (Martelli et al., 2002; Goto et al., 2006). Under both control and salt stress conditions, the ratio of nuclear ABA2 was higher in DGK5-OE plants but lower in dgk5-2 plants, which was consistent with the trend of nuclear PA levelsin DGK5-altered plants with or without salt stress. The minor effect of salt stress on the nuclear translocation of ABA2 might be due to the sampling timing of stress that is yet to be optimized. Our previous study showed that PA promotes heat-induced nuclear translocation of the cytosolic glycolytic enzyme glyceraldehyde-3-phosphate dehydrogenase (Kim et al., 2022). It might be possible that DGK5-derived PA associated with the nuclear membrane might

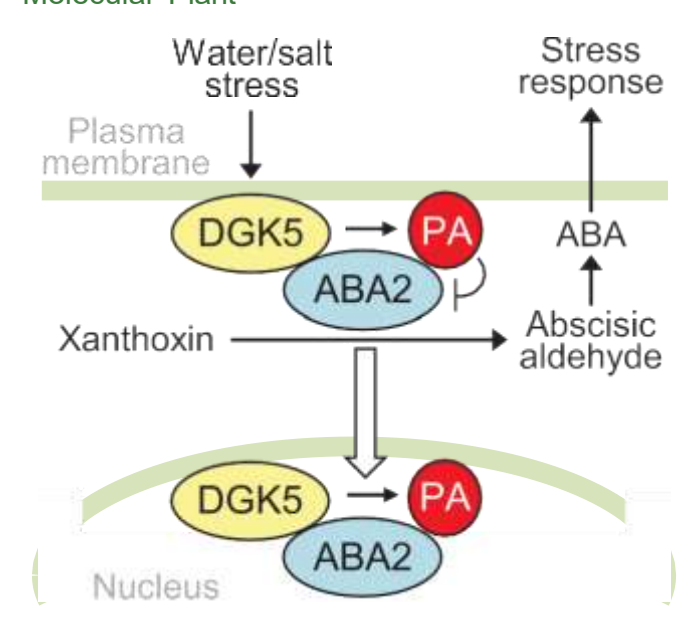


Figure 7. Model on DGK5-ABA2 interaction in ABA synthesis and stress response.

DGK5 and ABA2 are associated with one another in the nucleus and cytoplasm. DGK5 produces PA, which inhibits ABA2 dehydrogenase activity and decreases ABA production. The *dgk5* mutant decreases cellular and nuclear production of PA, alleviating ABA2 inhibition, so plants produce more ABA. Conversely, *DGK5*-OE increases cellular and nuclear production of PA, increasing PA inhibition of ABA2 activity and thus ABA production.

tether ABA2 to the nuclear membrane, facilitating its nuclear translocation. It is also conceivable that, like the PA-mediated nuclear translocation of glyceraldehyde-3-phosphate dehydrogenase (Kim et al., 2022), ABA2 associated with PA moves from the plasma membrane to the nucleus by vesicle trafficking Thus, DGK5 and PA suppress ABA production by both suppressing ABA2's enzymatic activity and promoting the nuclear sequestration of ABA2 (Figure 7).

The salt stress-induced PA increase is transient; it peaked at 30 min and then PA levels decreased even compared with nonstressed control plants. The transient PA increase under stress was also observed previously (Munnik et al., 2000; Yu et al., 2010). The decrease of total PA pool could result from a combination of decreases in de novo PA biosynthesis, total cellular phospholipid, other PA-generating reactions, such as PLD, as described below, and/or increases in PA catabolism. However, despite the PA decrease under stress, the dgk5 mutant and OE plants displayed lower and higher total and nuclear PA levels, respectively, than did WT, with a decrease in DAG in DGK5-OE plants. Those results indicate that the DGK5 activity contributes significantly to the total cellular and nuclear PA. In addition, the stress-induced DGK5 with increasing total cellular PA could mean that DGK5 affects specific pools of PA. For example, PA biosynthesized de novo is mostly associated with the endoplasmic reticulum. In nuclei, the PA changes may occur in nuclear envelope membranes and specific regions, such as nucleoplasm reticulum and/or nucleoplasm. Testing the multiple PA pools and their relevance with ABA2 interactions is a challenging future direction.

## Lipid phosphorylation interacts with ABA production

Besides DGKs, PLD is another major family of enzymes to produce the regulator PA by hydrolyzing membrane lipids (Hong et al., 2016; Ali et al., 2022). Previous studies indicate that PLDderived PA plays an important role in mediating ABA response (Zhang et al., 2004; Mishra et al., 2006; Li et al., 2019). The loss of PLDa1 decreased ABA- and stress-induced PA production associated with the plasma membrane and impeded ABApromoted stress response, such as stomatal closure and response to drought and salt stress (Zhang et al., 2004; Li et al., 2019). In addition, several other PLDs, including PLDa3, d ε, and zs, are involved in plant response to stress conditions, but none of those PLDs are associated with nuclei (Hong et al., 2016). However, our recent study showed that PA produced by PLDd that is associated with the plasma membrane increased heat-induced nuclear PA levels (Kim et al., 2022). The present study indicates that DGK5-derived PA binds to ABA2 and inhibits its activity, decreasing ABA production. Therefore, the PA pools derived from extranuclear PLDs may have a different effect from the PA that DGK5 produces primarily in nuclei. We propose that PLD-derived PA outside nuclear membranes, such as plasma membrane, mediates ABA signaling, whereas DGK5derived PA in nuclei suppresses ABA production.

In addition to different subcellular locations of PA produced, the different PA effects may also result from protein binding preference to different PA species. PA is comprised of various molecular species due to the carbon chain length and number of double bonds of two fatty acyl chains. For example, ABA-INSENSITIVE 1 (ABI1) in ABA signaling binds to di-18:1-PA but not to di-16:0-PA (Zhang et al., 2004). This binding preference is in stark contrast with LATE ELONGATED HYPOCOTYLS (LHY), an MYB transcription factor in *Arabidopsis*, which binds 16:0-containing PA species (e.g., di-16:0, 16:0/18-PA) but not di-18:1-PA (Kim et al., 2019). By comparison, ABA2 binds to various PA species tested, including di-18:0-PA, di-18:1-PA, 16:0/18:2-PA, and di-16:0-PA. How precisely the PA produced from DGK5 and specific PLD reactions have distinguishable functions requires further investigations.

Furthermore, besides PA, the effect of DGK5 on DAG may further contribute to the change in ABA production and stress responses. DAG is a class of important cellular mediators in animal cells in which it binds to C1 domain-containing proteins, such as protein kinase C (PKC), novel PKC, and Ras guanine nucleotidereleasing protein (Sim et al., 2020). While the direct molecular targets of DAG are yet to be identified in plants, manipulations of DAG levels by altering DGKs and non-specific phospholipase Cs suggest that DAG has the opposite effects to PA on root architecture and stomatal aperture (Peters et al., 2010; 2014; Yuan et al., 2019). The increase and decrease of PA/DAG ratios, as affected by DGK5-OE and the dgk5 mutant, respectively, would lead to the opposite changes in ABA production and plant stress responses. This study showed that PA inhibits ABA2 by inhibiting its catalytic activity and nuclear sequestration, but the effect of DGK5-decreased DAG and PA/DAG homeostasis remains to be elucidated.

In summary, this study documents that DGK5 interacts with ABA2 and suppresses ABA production (Figure 7). DGK5 and its lipid product PA bind to ABA2. The DGK5/PA-ABA2 interactions inhibit ABA2 activity and, additionally, promote the nuclear

# Lipid phosphorylation interacts with ABA production

translocation of ABA2 (Figure 7). Together, those interactions decrease ABA production and modulate plant response to stress conditions, such as salinity and drought. The results reveal a mechanism by which DGK5 regulates plant stress responses and indicate an important role of nuclear PA and lipid phosphorylation in mediating plant stress responses.

## **METHODS**

#### Plant materials

Arabidopsis thaliana (Columbia ecotype Col-0) was used for all experiments and transgenic lines in this study. T-DNA insertional mutants dgk5-2 (SALK\_120348) and dgk5-3 (SALK\_092764) were obtained from ABRC Stock Center (https://abrc.osu.edu) and verified by PCR using the pairs of primers JLP286/198 and JLP197/198 (supplemental Table 1), respectively. ABA2 (AT1G52340) mutants aba2-1 (CS156; Le' on-Kloosterziel et al., 1996; Gonza' lez-Guzma' n et al., 2002) and aba2-2 (CS3834; Laby et al., 2000) were obtained from ABRC. Mutant seeds were initially selected on antibiotics-containing plates and mutant plants were verified by PCR using pairs of primers JLP319/320 for aba2-1 and JLP321/318 for aba2-2 (Cheng et al., 2014). The DGK5 and ABA2 double mutants dgk5/aba2 and DGK5-OE/aba2 were produced by crossing aba2-1 (or aba2-2) with dgk5-3 and DGK5-OE, respectively. The dgk5/aba2 and DGK5-OE/aba2 plants were identified by PCR using primers as described above (supplemental Table 1) and mutants homozygous at both alleles were used for further experiments.

### Growth conditions and stress treatments

Seeds of WT and *DGK5* and/or *ABA2*-altered mutants were surface-sterilized in ethanol and bleach for 10 min, respectively, and rinsed four times with sterile  $H_2O$ . Sterilized seeds were sown in Petri dishes containing a  $^1/_2$  Murashige and Skoog (MS) medium with agar after stratification for 3 days in the dark at  $^4$ C. Seeds in plates were germinated in a growth chamber for 3 days. Three-day-old seedlings were transferred to  $^1/_2$  MS agar plates without or with 75 mM NaCl, 100 mM NaCl, or 150 mM sorbitol. Plates were kept vertically in a growth chamber with a 16-h light/8-h dark cycle and at  $23^{\circ}$ C/ $21^{\circ}$ C under cool fluorescent white light (200 mmol/m²/s). After 7 days, seedlings were imaged for primary root measurements using ImageJ (https://imagej.net). Five to 7 biological repeats of each treatment and a total of 23–30 seedlings were measured for each genotype.

For liquid culture, *Arabidopsis* seeds were sterilized and stratified for 3 days in the dark at 4°C, and then about 50 seeds were sown in a tissue culture containing 6 ml liquid ½ MS. The plates were kept in a shaker (80 rpm) in a growth chamber with a 16-h light/8-h dark cycle and at 23°C/21°C under cool fluorescent white light (200 mmol/m²/s). The culture medium was replaced every 3 days for 2 weeks, and then treated with 0 (control) or 100 mM NaCl. Whole seedlings were harvested at 0, 0.5, 3, and 6 h after treatments. Lipids were extracted immediately from fresh seedlings, while some seedlings were immediately frozen in liquid nitrogen for ABA extraction. Five biological repeats of every treatment were used for each genotype. For seedlings grown in liquid ½ MS medium were treated with or without 100 mM NaCl for 10 h. More than 1 g of fresh roots was collected for each sample for

nuclear isolation, followed by lipid extraction and analysis using ESI-MS/MS as described previously (Cai et al., 2020; Kim et al., 2020).

For NaCl stress in soil, 3-week-old plants were sub-irrigated with 100 mM NaCl solution. Each plant in a tray was allowed 20-30 min for absorption three times a week. Control plants were watered with greenhouse tap water each time that NaCl was applied to the stress plants. After 14 days, plants were harvested to measure fresh weight. The relative dry weight was calculated based on the formula: relative dry weight = data treatment/data control 3 100%. For drought treatments, 2-week-old plants were withheld watering for 16 days, and the wilted rate of plants was counted. These water-deficit plants were rewatered, and the survival rate of plants was counted 3 days after rewatering. The average wilted and survival rates were calculated from five independent experiments (n = 12-19 plants per genotype in each independent experiment). For waterlogging, 3-week-old plants were over-watered to maintain 100% water-saturated soil and relative humidity for 14 days, and the fresh weight and dry weight were recorded.

Stomatal closure assay was conducted as described previously (Zhang et al., 2004; Peters et al., 2010). In brief, the fresh leaves of 5-week-old plants at similar developmental stages were harvested. The epidermal peels were incubated in a stomatal opening buffer (5 mM MES-KOH [pH 6.15], 30 mM KCl, and 1 mM CaCl<sub>2</sub>) at 23°C under cool white light (150 mmol/m<sup>2</sup>/s) for 3 h to ensure the opening of stomata. ABA was then added to the buffer to a final concentration of 50 mM. After 3 h of incubation, photos of epidermal peels were taken, and the stomatal aperture was measured using ImageJ. At least 85 stomata were measured for each genotype. For measurement of water loss, the fully expanded detached leaves from 5-week-old plants were exposed to cool white light at 23°C. Leaves were weighed at various time intervals. The loss of fresh weight (%), fresh weight relative to the initial fresh weight of the detached leaves, was used to indicate water loss. Three to four independent experiments were conducted.

### Plasmid construction and plant transformation

DGK5-OE lines were constructed by amplifying the genomic sequence of DGK5 by PCR using Col-0 Arabidopsis genomic DNA as a template and the pair of primers JLP143/144. All primers used for PCR amplification are listed in supplemental Table 1. The fragment was cloned into the p35S-Fast-eYFP vector at the 30 end of the eYFP coding sequence under the control of the 35S cauliflower mosaic virus promoter. The construct was introduced into Agrobacterium tumefaciens strain GV3101 and then transformed into Arabidopsis (Col-0) using the floral-dip method (Clough and Bent, 1998). Positive transgenic plants were screened for antibiotic resistance and confirmed by PCR using the forward primer (GCP169) in the 35S promoter region of the p35S-Fast-eYFP vector and the reverse primer (JLP170) in the 30 terminal region of DGK5 (supplemental Table 1). The production of YFP-Flag-DGK5 in OE lines was verified by immunoblotting with an anti-Flag antibody. To generate the activity-dead DGK5d, the plasmid p35S-YFP-Flag containing the full-length coding sequence of WT DGK5 was used as a template, and the G112A mutation

was generated by overlapping PCR with primers listed in supplemental Table 1.

### Genetic complementation

A 4915-bp genomic DNA fragment containing its native promoter (1286 bp upstream from the start codon) was amplified by PCR using primers JLP145/146 (supplemental Table 1) and cloned into the pEC291 vector. The constructs were transformed by floral dipping into the two mutants *dgk5-2* and *dgk5-3*. Homozygous complemented plants were confirmed by antibiotic resistance to hygromycin and further verified by PCR using a forward primer (GCP228) in the pEC291 vector and a reverse primer (JLP171) in the 30 terminal region.

# Coprecipitation of DGK5 and ABA2 expressed in *E. coli* and plants

GST-tagged DGK5 and His-tagged ABA2 were constructed by cloning the full coding sequences of DGK5 and ABA2 using the gene-specific primers (supplemental Table 1), and the cDNAs were inserted into pGEX4T-1 and pET-28a, respectively. The plasmids were transformed into E. coli BL21, and the expression of GST-DGK5 and His-ABA2 was induced by 0.2 mM isopropylb-d-thiogalactoside at 24°C for 12 h. Cells were harvested after centrifugation at 3600 g for 15 min and then resuspended in a PBS buffer. After sonication, cell lysates were centrifuged at 10 000 g for 20 min at 4°C. Glutathione resin (GenScript, L00206) was added to supernatants of GST only or GST-DGK5 cell lysates and then incubated at 4°C for 1 h with gentle rotation. GST and GST-DGK5-immobilized resin were washed with PBS three times and then incubated with the total soluble proteins extracted from E. coli cells expressing His-ABA2 at 4°C for 2 h with gentle rotation. After the resin was washed with PBS six times, pull-down proteins were subject to SDS-PAGE and transferred onto a polyvinylidene fluoride (PVDF) membrane. GST and GST-DGK5 were immunodetected with a horseradish peroxidase (HRP)-conjugated anti-GST antibody (1:6000 dilution, GenScript, A00866). His-ABA2 was immunodetected with an anti-His antibody (1:5000 dilution, GenScript, A00186) as the primary antibody and HRP-conjugated anti-mouse antibody (1:6000 dilution, GE Healthcare, NXA931) as the secondary antibody.

For co-immunoprecipitation of DGK5 and ABA2 from plants, the full coding sequences of DGK5 and ABA2 were cloned into p35S-YFP-Flag and p35S-CFP, respectively. The coding sequence of the HA tag was included in the ABA2 reverse primer (supplemental Table 1). The constructs were transformed into A. tumefaciens C58C1 strain. The overnight-grown agrobacterial cells were harvested and washed with 10 mM MES (pH 5.7) and 10 mM MgCl<sub>2</sub>. After the agrobacteria solution was diluted to OD<sub>600</sub> of 0.8 with the infiltration buffer (10 mM MES [pH 5.7], 10 mM MgCl<sub>2</sub>, and 100 mM acetosyringone), it was incubated at room temperature for 3 h. The agrobacteria solution was infiltrated into the leaves of 3-week-old tobacco, and the tobacco was transferred back to the growth chamber for 2 days. Total protein was extracted from tobacco leaves with an extraction buffer (50 mM Tris-HCl [pH 8.0], 150 mM NaCl, 10 mM EDTA, 1 mM PMSF, and 0.5% [v/v] Triton X-100) and then filtered through four layers of Miracloth. After centrifugation at 2000 g for 10 min at 4°C, the proteins were incubated with an anti-HA antibody (1:1000 dilution, Invitrogen, 26183) for 1 h at 4°C and then

### Lipid phosphorylation interacts with ABA production

incubated with protein A agarose for 2 h at  $4^{\circ}$ C. After the beads were washed with the extraction buffer five times, the immunoprecipitated proteins were subjected to SDS–PAGE and then transferred onto PVDF membranes. Proteins were immunodetected with an anti-HA or anti-Flag antibody (1:6000 dilution, Sigma, F7425) as the primary antibody and an HRP-conjugated anti-rabbit (1:6000 dilution, Invitrogen, 32260) or anti-mouse antibody as the secondary antibody.

### BiFC in Arabidopsis protoplasts

For BiFC, the full coding sequences of *DGK5* and *ABA2* were cloned into pSAT1-cEYFP-C1B and pSAT1-nYFP-C1 (Citovsky et al., 2006), respectively. The plasmids were transfected into protoplasts isolated from the leaves of 4-week-old *Arabidopsis* (Wu et al., 2009). After incubating under light at room temperature for 12 h, protoplasts were observed with a confocal microscope (Zeiss LSM 900).

# ABA2 activity assay

The short-chain alcohol dehydrogenase activity of ABA2 was assayed according to a previously described method with some modifications (Gonza´ lez-Guzma´ n et al., 2002). For the dosage effect of DGK5 and lipids on ABA2 activity, the dehydrogenase activity of ABA2 was assayed at 25°C using purified ABA2 expressed in *E. coli* and 100 mM K<sub>2</sub>HPO<sub>4</sub> (pH 7.2), 500 mM NAD<sup>+</sup>, 30 mM 3,5,5°-trimethylcyclohexanol, and different amounts of purified DGK5 proteins or lipids. For determination of  $V_{\text{max}}$  and  $K_{\text{m}}$ , ABA2 activity was assayed using 100 mM K<sub>2</sub> HPO<sub>4</sub> (pH 7.2), 1 mM NAD<sup>+</sup>, and different concentrations of 3,5,5°-trimethylcyclohexanol. The assay was monitored by an increase in A<sub>340</sub> due to the reduction of NAD<sup>+</sup> to NADH, and the absorbance at 340 nm was recorded every 3 min for 90 min using a Cytation3 plate reader (BioTek).

### Filter-lipid-binding assay and liposome-binding assay

The lipid-binding ability of ABA2 was tested by the filter-binding assay and liposome-binding assay according to the previously described method with some modifications (Kim et al., 2013). For the filter-binding assay, 5 mg of lipids dissolved in chloroform was spotted on the nitrocellulose membrane and then air-dried for 45 min. The membrane was blocked with 1% (w/v) fatty acid-free bovine serum albumin in TBST buffer (10 mM Tris–HCI [pH 7.4], 140 mM NaCl, 0.1% [v/v] Tween 20) at room temperature for 1 h and then washed with TBST three times. After incubation with purified ABA2 (1.5 mg/ml in TBST) at 4°C for 2 h, the membrane was washed with TBST three times. The proteins on the membrane were immunodetected using an anti-His antibody.

For the liposome-binding assay, 10 mmol of di-18:1 PC, di-18:1 PC/di-18:1 PA (molar ratio of 3:1), or di-18:1 PC/di-18:1 DAG (molar ratio of 3:1) were dried under a gentle stream of nitrogen gas and then rehydrated for 1 h with HBS buffer (20 mM HEPES [pH 7.5], 100 mM NaCl, 0.02% [w/v] sodium azide). The rehydrated lipids were sonicated until the solution became nearly clear and centrifuged at 50 000 g for 15 min. The liposome pellet was resuspended in a binding buffer (25 mM Tris–HCl [pH 7.5], 125 mM KCl, 1 mM DTT, 0.5 mM EDTA) and then incubated with 5 mg of purified ABA2 proteins at room temperature for 1 h. The liposome-bound proteins were harvested by centrifuging

### Lipid phosphorylation interacts with ABA production

at 16 000 g for 30 min, washed with the binding buffer three times, and resuspended in SDS-PAGE loading buffer for immunoblotting.

# Transient expression of ABA2 in WT and DGK5-altered *Arabidopsis* leaves

Agrobacterium-mediated transient transformation of Arabidopsis was performed according to a previously described method with some modifications (Zhang et al., 2020). In brief, agrobacteria transformed with p35S::ABA2-HA-CFP were grown in LB medium containing antibiotics and 100 mM acetosyringone at 28°C for 20 h. The agrobacteria were harvested and washed with 10 mM MgCl<sub>2</sub> and 100 mM acetosyringone. After dilution to OD<sub>600</sub> of 0.5 in infiltration buffer (1/4 MS [pH 6.0], 1% sucrose, 100 mM acetosyringone, 0.01% Silwet L-77), the agrobacteria were incubated at room temperature for 2 h and then infiltrated into the leaves of 3-week-old Arabidopsis. After being kept in the light for 1 h, the plants were placed in the dark at room temperature for 24 h and then transferred back to the growth chamber for another 2 days. Arabidopsis leaves were observed using a confocal microscope (Zeiss LSM 900). For salt treatment, the plants were transferred into 100 mM NaCl solution for 2 h, and then the leaves were observed with a confocal microscope. For lipid treatment, the leaves were incubated with 0.005% Silwet L-77 solution with or without 10 mM di-18:1 DAG or PA for 1 h and then observed with a confocal microscope.

### Subcellular localization of DGK5

Agrobacterium harboring the YFP-Flag-DGK5 construct was infiltrated into tobacco leaves to express the YFP-Flag-DGK5 protein. The infiltrated tobacco leaves were incubated in the dark for 12 h and then in a growth chamber for 24 or 36 h before observation under an inverted Zeiss LSM 900 confocal microscope (excitation source: argon ion laser at 488 nm and detection filters between 500 and 600 nm). For observation of DGK5 location by subcellular fractionation, proteins were extracted from 1-weekold seedlings (WT and transformed plants) using chilled buffer A (0.5 M sucrose, 1 mM spermidine, 4 mM spermine, 10 mM EDTA, 10 mM Tris-HCl [pH 7.6], and 80 mM KCl), according to a previously reported method (Yao et al., 2013; Kim et al., 2020). The homogenate was filtered through four layers of Miracloth and centrifuged at 3000 g for 5 min at 4°C. The supernatant was then centrifuged at 16 000 g for 30 min at 4°C, and the resultant supernatant was used as the cytosolic fraction. The pellet from 3000 g centrifugation was gently dispersed in a suspension buffer (50 mM Tris-HCI, 5 mM MgCl<sub>2</sub>, 10 mM b-mercaptoethanol, and 20% glycerol). The suspension was loaded on a discontinuous Percoll gradient composed of 2 ml of 40%, 60%, and 80% Percoll solution in buffer C (0.44 M sucrose, 25 mM Tris-HCl [pH 7.5], and 10 mM MgCl<sub>2</sub>) onto 2 ml of 2 M sucrose cushion. The gradients were centrifuged at 3000 g in a swing-bucket rotor for 45 min at 4°C. The band that appeared in the 80% Percoll layer above the 2 M sucrose was collected as the nuclear fraction. The nuclear fraction was rinsed twice with buffer A, centrifuged at 6000 g for 10 min at 4°C, and then resuspended in the nuclear suspension buffer.

For protein detection, 10 mg protein samples were loaded on 10% (v/v) SDS-PAGE gel after dissolving in SDS-PAGE loading buffer

and boiling for 10 min at 95°C. The proteins were transferred onto a PVDF membrane. After blocking into 5% (w/v) nonfat milk in TBST for 30 min and rinsing three times for 5 min with TBST, the membranes were incubated in an anti-Flag antibody (1:6000 dilution), an anti-PEPC antibody (1:2000 dilution, Rockland, 100-4163), or an anti-histone H3 antibody (1:2000 dilution, GenScript, A01502), respectively, overnight at 4°C, and then washed three times with TBST buffer. The membranes were incubated in an HRP-conjugated anti-rabbit antibody as the secondary antibody.

### RT-qPCR

Total RNA was extracted from 14-day-old seedlings using the Plant RNA Purification Reagent (Invitrogen) according to the manufacturer's instruction. Chromosomal DNA was digested with RNase-free DNase (Ambion) according to the manufacturer's instructions. One microgram of total RNA was reverse transcribed into cDNA using an iScript cDNA Synthesis Kit (Bio-Rad, Hercules, CA). RT–qPCR was performed using SYBR Green to monitor the expression of the target and reference genes with an MyiQ Sequence Detection System (Bio-Rad). Melting curve analyses were performed for all samples by elevating the temperature from 55°C to 95°C. Transcript levels were normalized to the level of UBQ10 (Li et al., 2011). Fold change in expression of the target gene was calculated using the (1 + E)<sup>D(DCP)</sup> method (Pfaffl, 2001). The primer information for the RT–qPCR is listed in supplemental Table 1.

### Lipid extraction and profiling

Lipids were extracted and quantified as described previously (Welti et al., 2002). In brief, the seedlings of WT, the dgk5 mutant, and OE lines were grown vertically in plates with 1/2 MS liquid medium for 14 days. The roots of seedlings were collected and immersed immediately into 3 ml of pre-heated (75°C) isopropanol with 0.01% (v/v) butylated hydroxytoluene for 15 min. Lipids were extracted at least three times from samples using chloroform/methanol (2:1, v/v). The extracted lipids were rinsed twice with 1 M KCl and once with water. The remaining tissues were dried in an oven at 100°C for 2 days and weighed. The lipids were dried with nitrogen and diluted in chloroform accordingly to the dry weight of the samples. The lipid extract was combined with solvents, chloroform/methanol/ ammonium acetate (300 mM) in water (300:665:35, v/v/v) and internal standards, and then detected by ESI-MS/MS. Lipid levels were calculated by comparison with internal standards, and the lipid contents were normalized to the sample dry weight (Li et al., 2006) or nuclear protein. DAG was quantified by a series of neutral loss scans that detected DAG species as [M + NH<sub>4</sub>]<sup>+</sup> ions (Peters et al., 2010; Yuan et al., 2019). The corrected signals based on each DAG species were combined, and the levels of DAG species were quantified according to the internal standard (di-15:0-DAG). As there are varied ionization and fragmentation efficiencies among different acyl groups, the contents of DAG species were expressed as mass spectral signal relative to the internal standard.

### ABA measurements

ABA content was determined according to the previous study with some modifications as detailed below (Pan et al., 2010). Arabidopsis leaves were frozen immediately and ground into

powder. Endogenous ABA was extracted using an extraction buffer, isopropanol/ $H_2O$ /concentrated HCI (2:1:0.002, v/v/v). Twenty-five nanograms of d6-ABA (Icon Isotopes, ID1001) was added to each sample. After shaking at 4°C for 30 min, the mixture was added with 800 ml of dichloromethane and shaken for 30 min at 4°C. The lower phase was transferred to a clean tube after centrifuging at 13 000 g for 5 min at 4°C. The diluted sample was determined using HPLC–ESI-MS/MS (Thermo Fisher TSQ Altis).

### Statistical analysis

For multiple comparisons, data were analyzed by one-way ANOVA. For statistical differences between means, data were analyzed using Student's *t*-test.

## **ACCESSION NUMBERS**

Sequence data from this article can be found in the Arabidopsis Genome Initiative database under the following accession numbers: *DGK5*, AT2G20900; *UBQ10*, At4g05320; *ABA2*, AT1G52340; *ABI1*, AT4G26080; *ABA3*, AT1G16540; *AtNCED3*, AT3G14440. The numbers for T-DNA insertion are as follows: *dgk5-2*, SALK\_120348; *dgk5-3*, SALK\_092764. EMS mutants are *aba2-1*, Cs156 and *aba2-2*, CS3834.

### SUPPLEMENTAL INFORMATION

Supplemental information is available at Molecular Plant Online.

#### **FUNDING**

Research reported in this article was supported by the National Institute of General Medical Sciences of the National Institutes of Health under award number R01GM141374 and the National Science Foundation grants 2222157 and 2302424.

### **AUTHOR CONTRIBUTIONS**

J.L. and S.Y. designed and performed the experiments and wrote the manuscript. S.-C.K. assisted on nuclear isolation and analysis. X.W. proposed and supervised the study and revised the manuscript. All authors discussed the results and commented on the manuscript.

### **ACKNOWLEDGMENTS**

No conflict of interest to declare.

Received: July 27, 2023 Revised: December 8, 2023 Accepted: January 5, 2024 Published: January 19, 2024

### **REFERENCES**

- Ali, U., Lu, S., Fadlalla, T., Iqbal, S., Yue, H., Yang, B., Hong, Y., Wang, X., and Guo, L. (2022). The functions of phospholipases and their hydrolysis products in plant growth, development and stress responses. Prog. Lipid Res. 86, 101158.
- Angkawijaya, A.E., Nguyen, V.C., Gunawan, F., and Nakamura, Y. (2020). A Pair of Arabidopsis Diacylglycerol Kinases Essential for Gametogenesis and Endoplasmic Reticulum Phospholipid Metabolism in Leaves and Flowers. Plant Cell 32:2602–2620.
- Arabidopsis Interactome Mapping Consortium. (2011). Evidence for network evolution in an Arabidopsis interactome map. Science 333:601–607.
- Bozelli, J.C., Jr., and Epand, R.M. (2022). DGKa, Bridging Membrane Shape Changes with Specific Molecular Species of DAG/PA: Implications in Cancer and Immunosurveillance. Cancers 14:5259.

### Lipid phosphorylation interacts with ABA production

- Cacas, J.L., Gerbeau-Pissot, P., Fromentin, J., Cantrel, C., Thomas, D., Jeannette, E., Kalachova, T., Mongrand, S., Simon-Plas, F., and Ruelland, E. (2017). Diacylglycerol kinases activate tobacco NADPH oxidase-dependent oxidative burst in response to cryptogein. Plant Cell Environ. 40:585–598.
- Cai, G., Kim, S.C., Li, J., Zhou, Y., and Wang, X. (2020). Transcriptional Regulation of Lipid Catabolism during Seedling Establishment. Mol. Plant 13:984–1000.
- Cheng, W.H., Endo, A., Zhou, L., Penney, J., Chen, H.C., Arroyo, A., Leon, P., Nambara, E., Asami, T., Seo, M., et al. (2002). A unique short-chain dehydrogenase/reductase in Arabidopsis glucose signaling and abscisic acid biosynthesis and functions. Plant Cell 14:2723–2743.
- Cheng, Z.J., Zhao, X.Y., Shao, X.X., Wang, F., Zhou, C., Liu, Y.G., Zhang, Y., and Zhang, X.S. (2014). Abscisic acid regulates early seed development in Arabidopsis by ABI5-mediated transcription of SHORT HYPOCOTYL UNDER BLUE1. Plant Cell 26:1053–1068.
- Chibalin, A.V., Leng, Y., Vieira, E., Krook, A., Bjo€rnholm, M., Long, Y.C., Kotova, O., Zhong, Z., Sakane, F., Steiler, T., et al. (2008). Downregulation of diacylglycerol kinase delta contributes to hyperglycemia-induced insulin resistance. Cell 132:375–386.
- Citovsky, V., Lee, L.Y., Vyas, S., Glick, E., Chen, M.H., Vainstein, A., Gafni, Y., Gelvin, S.B., and Tzfira, T. (2006). Subcellular localization of interacting proteins by bimolecular fluorescence complementation in planta. J. Mol. Biol. 362:1120–1131.
- Clough, S.J., and Bent, A.F. (1998). Floral dip: a simplified method for Agrobacterium-mediated transformation of Arabidopsis thaliana. Plant J. 16:735–743.
- de Torres-Zabala, M., Truman, W., Bennett, M.H., Lafforgue, G., Mansfield, J.W., Rodriguez Egea, P., Bo€gre, L., and Grant, M. (2007). Pseudomonas syringae pv. tomato hijacks the Arabidopsis abscisic acid signalling pathway to cause disease. EMBO J. 26:1434–1443.
- Dominguez, C.L., Floyd, D.H., Xiao, A., Mullins, G.R., Kefas, B.A., Xin, W., Yacur, M.N., Abounader, R., Lee, J.K., Wilson, G.M., et al. (2013). Diacylglycerol kinase a is a critical signaling node and novel therapeutic target in glioblastoma and other cancers. Cancer Discov. 3:782–797.
- Escobar-Sepu' Iveda, H.F., Trejo-Te' Ilez, L.I., Pe' rez-Rodri'guez, P., Hidalgo-Contreras, J.V., and Go' mez-Merino, F.C. (2017). Diacylglycerol Kinases Are Widespread in Higher Plants and Display Inducible Gene Expression in Response to Beneficial Elements, Metal, and Metalloid Ions. Front. Plant Sci. 8:129.
- Frias, M.A., Hatipoglu, A., and Foster, D.A. (2023). Regulation of mTOR by phosphatidic acid. Trends Endocrinol. Metabol. 34:170–180.
- Ge, H., Chen, C., Jing, W., Zhang, Q., Wang, H., Wang, R., and Zhang, W. (2012). The rice diacylglycerol kinase family: functional analysis using transient RNA interference. Front. Plant Sci. 3:60.
- Go´ mez-Merino, F.C., Arana-Ceballos, F.A., Trejo-Te´ llez, L.I., Skirycz, A., Brearley, C.A., Do€rmann, P., and Mueller-Roeber, B. (2005). Arabidopsis AtDGK7, the smallest member of plant diacylglycerol kinases (DGKs), displays unique biochemical features and saturates at low substrate concentration: the DGK inhibitor R59022 differentially affects AtDGK2 and AtDGK7 activity in vitro and alters plant growth and development. J. Biol. Chem. 280:34888–34899.
- Gonza´ lez-Guzma´ n, M., Apostolova, N., Belle´ s, J.M., Barrero, J.M., Piqueras, P., Ponce, M.R., Micol, J.L., Serrano, R., and Rodrı´guez, P.L. (2002). The short-chain alcohol dehydrogenase ABA2 catalyzes the conversion of xanthoxin to abscisic aldehyde. Plant Cell 14:1833–1846.

- Goto, K., Hozumi, Y., and Kondo, H. (2006). Diacylglycerol, phosphatidic acid, and the converting enzyme, diacylglycerol kinase, in the nucleus. Biochim. Biophys. Acta 1761:535–541.
- Hong, Y., Zhao, J., Guo, L., Kim, S.C., Deng, X., Wang, G., Zhang, G., Li, M., and Wang, X. (2016). Plant phospholipases D and C and their diverse functions in stress responses. Prog. Lipid Res. 62:55–74.
- Jia, K.P., Mi, J., Ali, S., Ohyanagi, H., Moreno, J.C., Ablazov, A., Balakrishna, A., Berqdar, L., Fiore, A., Diretto, G., et al. (2022). An alternative, zeaxanthin epoxidase-independent abscisic acid biosynthetic pathway in plants. Mol. Plant 15:151–166.
- Kalachova, T., S~kraba´ Ikova´, E., Pateyron, S., Soubigou-Taconnat, L., Djafi, N., Collin, S., Sekeres~, J., Burketova´, L., Potocky´, M., Pejchar, P., et al. (2022). DIACYLGLYCEROL KINASE 5 participates in flagellin-induced signaling in Arabidopsis. Plant Physiol. 190:1978–1996
- Kim, S.C., Guo, L., and Wang, X. (2013). Phosphatidic acid binds to cytosolic glyceraldehyde-3-phosphate dehydrogenase and promotes its cleavage in Arabidopsis. J. Biol. Chem. 288:11834–11844.
- Kim, S.C., Guo, L., and Wang, X. (2020). Nuclear moonlighting of cytosolic glyceraldehyde-3-phosphate dehydrogenase regulates Arabidopsis response to heat stress. Nat. Commun. 11:3439.
- Kim, S.C., Nusinow, D.A., Sorkin, M.L., Pruneda-Paz, J., and Wang, X. (2019). Interaction and Regulation Between Lipid Mediator Phosphatidic Acid and Circadian Clock Regulators. Plant Cell 31:399–416.
- Kim, S.C., Yao, S., Zhang, Q., and Wang, X. (2022). Phospholipase Dd and phosphatidic acid mediate heat-induced nuclear localization of glyceraldehyde-3-phosphate dehydrogenase in Arabidopsis. Plant J. 112:786–799.
- Kim, S.C., and Wang, X. (2020). Phosphatidic acid: an emerging versatile class of cellular mediators. Essays Biochem. 64:533–546.
- Kolesnikov, Y., Kretynin, S., Bukhonska, Y., Pokotylo, I., Ruelland, E., Martinec, J., and Kravets, V. (2022). Phosphatidic Acid in Plant Hormonal Signaling: From Target Proteins to Membrane Conformations. Int. J. Mol. Sci. 23:3227.
- Laby, R.J., Kincaid, M.S., Kim, D., and Gibson, S.I. (2000). The Arabidopsis sugar-insensitive mutants sis4 and sis5 are defective in abscisic acid synthesis and response. Plant J. 23:587–596.
- Le´ on-Kloosterziel, K.M., Gil, M.A., Ruijs, G.J., Jacobsen, S.E., Olszewski, N.E., Schwartz, S.H., Zeevaart, J.A., and Koornneef, M. (1996). Isolation and characterization of abscisic acid-deficient Arabidopsis mutants at two new loci. Plant J. 10:655–661.
- Li, M., Bahn, S.C., Guo, L., Musgrave, W., Berg, H., Welti, R., and Wang, X. (2011). Patatin-related phospholipase pPLAIIIb-induced changes in lipid metabolism alter cellulose content and cell elongation in Arabidopsis. Plant Cell 23:1107–1123.
- Li, M., Qin, C., Welti, R., and Wang, X. (2006). Double knockouts of phospholipases Dzeta1 and Dzeta2 in Arabidopsis affect root elongation during phosphate-limited growth but do not affect root hair patterning. Plant Physiol. 140:761–770.
- Li, T., Xiao, X., Liu, Q., Li, W., Li, L., Zhang, W., Munnik, T., Wang, X., and Zhang, Q. (2023). Dynamic responses of PA to environmental stimuli imaged by a genetically encoded mobilizable fluorescent sensor. Plant Commun. 4, 100500.
- Li, W., Song, T., Wallrad, L., Kudla, J., Wang, X., and Zhang, W. (2019). Tissue-specific accumulation of pH-sensing phosphatidic acid determines plant stress tolerance. Nat. Plants 5:1012–1021.
- Li, Y., Wang, M., Guo, T., Li, S., Teng, K., Dong, D., Liu, Z., Jia, C., Chao, Y., and Han, L. (2022). Overexpression of *abscisic acid-insensitive gene ABI4* from *Medicago truncatula*, which could interact with ABA2, improved plant cold tolerance mediated by ABA signaling. Front. Plant Sci. 13, 982715.

- Lin, P.C., Hwang, S.G., Endo, A., Okamoto, M., Koshiba, T., and Cheng, W.H. (2007). Ectopic expression of ABSCISIC ACID 2/GLUCOSE INSENSITIVE 1 in Arabidopsis promotes seed dormancy and stress tolerance. Plant Physiol. 143:745–758.
- Martelli, A.M., Bortul, R., Tabellini, G., Bareggi, R., Manzoli, L., Narducci, P., and Cocco, L. (2002). Diacylglycerol kinases in nuclear lipid-dependent signal transduction pathways. Cell. Mol. Life Sci. 59:1129–1137.
- Mishra, G., Zhang, W., Deng, F., Zhao, J., and Wang, X. (2006). A bifurcating pathway directs abscisic acid effects on stomatal closure and opening in Arabidopsis. Science 312:264–266.
- Munnik, T., Meijer, H.J., Ter Riet, B., Hirt, H., Frank, W., Bartels, D., and Musgrave, A. (2000). Hyperosmotic stress stimulates phospholipase D activity and elevates the levels of phosphatidic acid and diacylglycerol pyrophosphate. Plant J. 22:147–154.
- Pan, X., Welti, R., and Wang, X. (2010). Quantitative analysis of major plant hormones in crude plant extracts by high-performance liquid chromatography-mass spectrometry. Nat. Protoc. 5:986–992.
- Peters, C., Li, M., Narasimhan, R., Roth, M., Welti, R., and Wang, X. (2010). Nonspecific phospholipase C NPC4 promotes responses to abscisic acid and tolerance to hyperosmotic stress in Arabidopsis. Plant Cell 22:2642–2659.
- Peters, C., Kim, S.C., Devaiah, S., Li, M., and Wang, X. (2014). Non-specific phospholipase C5 and diacylglycerol promote lateral root development under mild salt stress in Arabidopsis. Plant Cell Environ. 37:2002–2013.
- Pfaffl, M.W. (2001). A new mathematical model for relative quantification in real-time RT-PCR. Nucleic Acids Res. 29:e45.
- Rook, F., Corke, F., Card, R., Munz, G., Smith, C., and Bevan, M.W. (2001). Impaired sucrose-induction mutants reveal the modulation of sugar-induced starch biosynthetic gene expression by abscisic acid signalling. Plant J. 26:421–433.
- Sakane, F., Hoshino, F., Ebina, M., Sakai, H., and Takahashi, D. (2021). The Roles of Diacylglycerol Kinase a in Cancer Cell Proliferation and Apoptosis. Cancers 13:5190.
- Scholz, P., Pejchar, P., Fernkorn, M., S~kraba´ Ikova´, E., Pleskot, R., Blersch, K., Munnik, T., Potocky´, M., and Ischebeck, T. (2022). DIACYLGLYCEROL KINASE 5 regulates polar tip growth of tobacco pollen tubes. New Phytol. 233:2185–2202.
- Sim, J.A., Kim, J., and Yang, D. (2020). Beyond Lipid Signaling: Pleiotropic Effects of Diacylglycerol Kinases in Cellular Signaling. Int. J. Mol. Sci. 21:6861.
- Tan, W.J., Yang, Y.C., Zhou, Y., Huang, L.P., Xu, L., Chen, Q.F., Yu, L.J., and Xiao, S. (2018). DIACYLGLYCEROL ACYLTRANSFERASE and DIACYLGLYCEROL KINASE Modulate Triacylglycerol and Phosphatidic Acid Production in the Plant Response to Freezing Stress. Plant Physiol. 177:1303–1318.
- Tang, F., Xiao, Z., Sun, F., Shen, S., Chen, S., Chen, R., Zhu, M., Zhang, Q., Du, H., Lu, K., et al. (2020). Genome-wide identification and comparative analysis of diacylglycerol kinase (DGK) gene family and their expression profiling in Brassica napus under abiotic stress. BMC Plant Biol. 20:473.
- Vu, H.S., Shiva, S., Roth, M.R., Tamura, P., Zheng, L., Li, M., Sarowar, S., Honey, S., McEllhiney, D., Hinkes, P., et al. (2014). Lipid changes after leaf wounding in Arabidopsis thaliana: expanded lipidomic data form the basis for lipid co-occurrence analysis. Plant J. 80:728–743.
- Welti, R., Li, W., Li, M., Sang, Y., Biesiada, H., Zhou, H.E., Rajashekar, C.B., Williams, T.D., and Wang, X. (2002). Profiling membrane lipids in plant stress responses. Role of phospholipase D alpha in freezing-induced lipid changes in Arabidopsis. J. Biol. Chem. 277:31994–32002

- Wong, A., Donaldson, L., Portes, M.T., Eppinger, J., Feijo´, J.A., and Gehring, C. (2020). *Arabidopsis* DIACYLGLYCEROL KINASE4 is involved in nitric oxide-dependent pollen tube guidance and fertilization. Development 147:dev183715.
- Wu, F.H., Shen, S.C., Lee, L.Y., Lee, S.H., Chan, M.T., and Lin, C.S. (2009). Tape-Arabidopsis Sandwich - a simpler Arabidopsis protoplast isolation method. Plant Methods 5:16.
- Yao, H., Wang, G., Guo, L., and Wang, X. (2013). Phosphatidic acid interacts with a MYB transcription factor and regulates its nuclear localization and function in Arabidopsis. Plant Cell 25:5030–5042.
- Yuan, S., Kim, S.C., Deng, X., Hong, Y., and Wang, X. (2019). Diacylglycerol kinase and associated lipid mediators modulate rice root architecture. New Phytol. 223:261–276.
- Yu, L., Nie, J., Cao, C., Jin, Y., Yan, M., Wang, F., Liu, J., Xiao, Y., Liang, Y., and Zhang, W. (2010). Phosphatidic acid mediates salt stress response by regulation of MPK6 in Arabidopsis thaliana. New Phytol. 188:762–773.

# Lipid phosphorylation interacts with ABA production

- Zha, Y., Marks, R., Ho, A.W., Peterson, A.C., Janardhan, S., Brown, I., Praveen, K., Stang, S., Stone, J.C., and Gajewski, T.F. (2006). T cell anergy is reversed by active Ras and is regulated by diacylglycerol kinase-alpha. Nat. Immunol. 7:1166–1173.
- Zhang, W., Qin, C., Zhao, J., and Wang, X. (2004). Phospholipase D alpha 1-derived phosphatidic acid interacts with ABI1 phosphatase 2C and regulates abscisic acid signaling. Proc. Natl. Acad. Sci. USA 101:9508–9513.
- Zhang, Y., Chen, M., Siemiatkowska, B., Toleco, M.R., Jing, Y., Strotmann, V., Zhang, J., Stahl, Y., and Fernie, A.R. (2020). A Highly Efficient Agrobacterium-Mediated Method for Transient Gene Expression and Functional Studies in Multiple Plant Species. Plant Commun. 1, 100028.
- Zhang, Y., Zhu, H., Zhang, Q., Li, M., Yan, M., Wang, R., Wang, L., Welti, R., Zhang, W., and Wang, X. (2009). Phospholipase dalpha1 and phosphatidic acid regulate NADPH oxidase activity and production of reactive oxygen species in ABA-mediated stomatal closure in Arabidopsis. Plant Cell 21:2357–2377.